Aus dem Institut für Molekulare Kardiologie
der Heinrich-Heine-Universität Düsseldorf
Kommissarische Institutsleitung: Prof. Dr. rer. nat. Ulrich Flögel

The Effect of Gender on Angiotensin II-Induced Aortic Disease in Mice with CD73 Deficiency

Dissertation

zur Erlangung des Grades eines Doktors der Zahnmedizin
der Medizinischen Fakultät der Heinrich-Heine-Universität Düsseldorf

vorgelegt von

Fady Ibrahim

2024

Als Inauguraldissertation gedruckt mit der Genehmigung der
Medizinischen Fakultät der Heinrich-Heine-Universität Düsseldorf

gez.:
Dekan: Prof. Dr. med. Nikolaj Klöcker
Erstgutachter: Prof. Dr. Ulrich Flögel
Zweitgutachter: PD. Dr. Sebastian Temme

To my parents, departed grandparents, family, and friends

‘For God has not given us a spirit of fear, but of power and of love and of a sound mind’

Parts of this work have been published:

Massold T, **Ibrahim F**, Niemann V, Steckel B, Becker K, Schrader J, Stegbauer J, Temme S, Grandoch M, Flögel U, Bouvain P. CD73 deficiency does not aggravate angiotensin II-induced aortic inflammation in mice. Scientific Reports volume 13, Article number: 17125 (2023) Oct 10. doi: 10.1038/s41598-023-44361-7. PMID: 37816827

1. Zusammenfassung

Die Entstehung von Bauchaortenaneurysmen (AAA) wird maßgeblich von vaskulärer Entzündung beeinflusst. Obwohl AAA im Falle eines Risses mit hoher Mortalitätsgefahr verbunden sind, gibt es derzeit nur wenige wirksame Behandlungen, weshalb neue therapeutische Ansatzpunkte erforderlich sind. Eine Ecto-5'-Nukleotidase, bekannt als CD73, die Adenosin produziert, könnte ein potenzielles neues Ziel sein. Seine regulatorische Rolle bei chronischen entzündlichen Erkrankungen, deutet auf seine Relevanz bei vaskulären Entzündungen hin und auf seine potenzielle Nützlichkeit als pharamkologisches Ziel zur Behandlung von AAA. In dieser Studie postulieren wir die Hypothese, dass ein Mangel an CD73 und folglich an Adenosin zu einer gesteigerten vaskulären Entzündung führt. Demzufolge könnte CD73 eine vielversprechende Zielstruktur für die medikamentöse Behandlung von AAA darstellen.

Die vaskuläre Entzündung wurde durch Angiotensin II (Ang II) induziert. Hierzu wurden osmotische Minipumpen subkutan implantiert, die über einen Zeitraum von 10 Tagen kontinuierlich Ang II in $CD73^{+/+}$ und $CD73^{-/-}$ Mäuse infundierten. Die Mäuse wurden vor und nach der Ang II-Infusion mittels Magnetresonanztomographie (MRT) und Ultraschall untersucht, um Informationen über die morphologischen sowie funktionellen Eigenschaften ihrer Aorten, wie z. B. den Lumina-Bereich, die Wandspannung (Strain) und die Blutflussgeschwindigkeit, zu erhalten. Zusätzlich wurde die Immunzellverteilung in der Aorta mittels Durchflusszytometrie vor und nach der Ang II-Infusion untersucht. Wir untersuchten auch die Auswirkungen von Ang II bei weiblichen und männlichen Mäusen, da das Geschlecht ein wesentlicher Faktor ist, der mit der Entwicklung von AAA verbunden ist.

Zwischen $CD73^{+/+}$ und $CD73^{-/-}$ Mäusen bestand kein Unterschied in der Anzahl der Immunzellen weder vor noch nach der Ang II-Infusion. Das Geschlecht hatte keinen Einfluss auf diese Ergebnisse. Zwischen $CD73^{+/+}$ und $CD73^{-/-}$ Mäusen bestand kein erkennbarer Unterschied im Gefäßbereich, der Wandspannung oder der Blutflussgeschwindigkeit, die morphologische und funktionelle Merkmale darstellen. Interessanterweise nahm während der Ang II-Infusion die Expression von CD73 bei $CD73^{+/+}$ Mäusen dramatisch ab.

Innerhalb der begrenzten Rahmenbedingungen dieser Studie konnten wir keine eindeutigen Belege dafür finden, dass das Fehlen von CD73 zu einer erhöhten vaskulären Entzündung führt. Die Auswirkungen von CD73 auf die Gefäßentzündung werden nicht durch das Geschlecht beeinflusst. Die Behandlung mit Ang II führte zu einem signifikanten Rückgang der CD73-Expression, unabhängig vom Geschlecht. Daher könnte die gezielte Erhöhung von CD73 als pharmakologisches Ziel dazu beitragen, die vaskuläre Entzündung zu verringern. Weitere Forschung ist jedoch erforderlich, um diese Hypothese weiter zu untersuchen.

2. Summary

The pathogenesis of abdominal aortic aneurysms (AAA) is strongly associated with vascular inflammation, presenting a critical challenge due to the high mortality risk associated with ruptures and limited treatment options. Identification of novel therapeutic targets is thus imperative. CD73, an ecto-5′-nucleotidase enzyme involved in adenosine production, emerges as a potential candidate. Its regulatory role in chronic inflammatory diseases suggests its relevance in vascular inflammation and potential utility as a pharmacological target for AAA treatment. In this study, we hypothesize that a deficiency of CD73 and consequently of adenosine leads to increased vascular inflammation. Therefore, CD73 could represent a promising target for the pharmacological treatment of AAA.

To investigate this hypothesis, we induced vascular inflammation in $CD73^{+/+}$ and $CD73^{-/-}$ mice via infusion of Angiotensin II (Ang II) over a 10-day period using osmotic minipumps. Magnetic resonance imaging (MRI) and ultrasound assessments were conducted pre- and post-infusion to assess morphological and functional changes in the aorta, including luminal area, wall strain, and blood flow velocity. Additionally, flow cytometry analysis was employed to evaluate immune cell distribution and ectoenzyme expression on immune cells before and after Ang II infusion. Gender differences were also explored, given their relevance to AAA development.

Our findings revealed no significant difference in immune cell infiltration between $CD73^{+/+}$ and $CD73^{-/-}$ mice, irrespective of Ang II infusion. Gender did not impact these outcomes. Moreover, there were no discernible differences in morphological and functional parameters such as vessel area, wall strain, and blood flow velocity between $CD73^{+/+}$ and $CD73^{-/-}$ mice. Notably, CD73 expression decreased significantly in $CD73^{+/+}$ mice during Ang II infusion.

While our study presents limitations, including the inability to definitively establish the role of CD73 in vascular inflammation and the lack of sex-dependent effects, the observed decline in CD73 expression suggests its potential as a therapeutic target. Further research is needed to elucidate the precise mechanisms and therapeutic implications of modulating CD73 activity in AAA management.

3. List of Abbreviations:

AAA	Abdominal Aortic Aneurysm
ACE	Angiotensin-Converting-Enzyme
Ado	Adenosin
ADP	Adenosin Diphosphate
AMP	Adenosin Monophosphate
Ang II	Angiotensin II
APC	Antigen Presenting Cells
ATP	Adenosin Triphosphate
ATR 1/2	Angiotensin II Receptors
BL	Baseline
CCR2	C-C Chemokine Receptor type 2
CCR7	C-C Chemokine Receptor type 7
CD	Cluster of Differentiation
COPD	Chronic Obstructive Pulmonary Disease
CT	Computed Tomography
DAPI	4′,6-diamidino-2-phenylindole
ECG	Electrocardiodiagram
ENPP1	Ectonucleotide Pyrophosphatase/Phosphodiesterase 1
ESAM	Endothelial cell-selective adhesion molecule

EVAR	Endovascular Aneurysm Repair
FACs	Fluorescence Activated Cell Sorting
ICAM 1	Intercellular adhesion molecule-1
IFN	Interferon
IL	Interleukin
LANUV	Landesamt für Natur-, Umwelt- und Verbraucherschutz
MCP-1	Monocyte Chemoattractant Protein-1
MHC	Major Histocompatibility Complex
MRI	Magentic Resonance Imaging
NAD	Nicotinamide Adenine Dinucleotide
NADH	Nicotinamide Adenine Dinucleotide Hydrogen
NADPH	Nicotinamide Adenine Dinucleotide Phosphate Hydrogen
NET	Neutrophil Extracellular Traps
NF-κB	Nuclear Factor Kappa
NMR	Nuclear Magnetic Resonance
NO	Nitric Oxide
PBS	Phosphate Buffered Saline
PET	Positron Emission Tomography
RAAS	Renin–Angiotensin–Aldosterone System
ROS	Reactive Oxygen Species
RPMI	Rosewell Park Memorial Institute Medium

SPECT	Single Photon Emission Computed Tomography
TNF	Tumor Necrosis Factor
VCAM1	Vascular cell adhesion molecule-1

4. Table of Contents

5. Introduction:

5.1 Abdominal Aortic Aneurysms

Abdominal aortic aneurysms (AAAs) are chronic diseases of multifactorial genesis, defined by an enlargement of the vessel diameter to either over 50 % of its normal diameter or 30 mm or more in the infrarenal area, whether in the anteroposterior or transverse plane (Moll et al., 2011, Johnston et al., 1991). While many different manipulable factors (such as high blood pressure, obesity, smoking) and non-manipulable factors (such as older age, male sex, family history) are known to increase the risk of developing an AAA (Kent et al., 2010, Kim et al., 2023, Altobelli et al., 2018, Cornuz et al., 2004), the exact effect and individual contribution of these biological factors, as well as the extent to which they play a role in the unfortunate event of an AAA rupture, remain unclear (Krishna et al., 2020). One of the known factors for the formation of AAAs is caused by modifications in the aortic wall. The so-called vascular inflammation, which leads to the thinning of media and adventitia due to the degradation of the extracellular matrix, collagen and elastic fibers, and therefore loss of smooth muscle cells, further weakens the aorta and makes it more susceptible to the formation of an AAA (Kuivaniemi et al., 2015, Dale et al., 2015). The immune cells and their products promote further damage and weakness of the vessel wall (Sakalihasan et al., 2005), and due to the luminal blood pressure, a bulging of the aorta is forced. Atherosclerosis, hypertension, or other factors might cause further dilation of the already weakened vessel wall, leading to a rupture of the vessel, which is associated with a mortality rate of up to 80 % (Golledge and Norman, 2010, Filardo et al., 2015, Tada et al., 2014). Figure 5-1 depicts the rough anatomical landmarks and different forms of AAAs. They often occur infrarenally and may take several other forms. Depending on the defect, they can be classified as dissecting aneurysms (tear in the intimal layer and separation of the arterial wall layers with formation of a second lumen), false aneurysms (perforation of the vessel wall with formation of an extravascular hematoma), or true aneurysms (involvement of all three layers). Although AAA is associated with this high risk of mortality and is essentially a medical emergency, treatments are still limited, and immediate aortic surgery is the only lifesaving option. In a study analyzing the in-hospital mortality rates of surgically

treated patients after the rupture of an AAA, it was shown that the mortality rates were approximately 44% (Kühnl et al., 2017). As AAAs typically grow asymptomatically, their diagnosis often occurs incidentally during routine ultrasound examinations, which are accurate and reliable, given the poor prognosis in the event of rupture (Fleming et al., 2005). The majority of AAAs discovered during screening are modest (29 to 49 mm in diameter); just 0.4% to 0.6% of the population are screened for AAAs larger than 55 mm (Von Allmen and Powell, 2012). The risk of rupture increases with larger diameters, and at certain diameters, surgery should be performed, however still leaving a perioperative mortality risk ranging from 4 to 8 % (Brown et al., 2012). Currently, there are not many satisfactory pharmaceutical therapies available. Therefore, new pharmaceutical targets need to be found to prevent vascular inflammation, thereby inhibiting AAA growth and rupture (Charo and Taub, 2011).

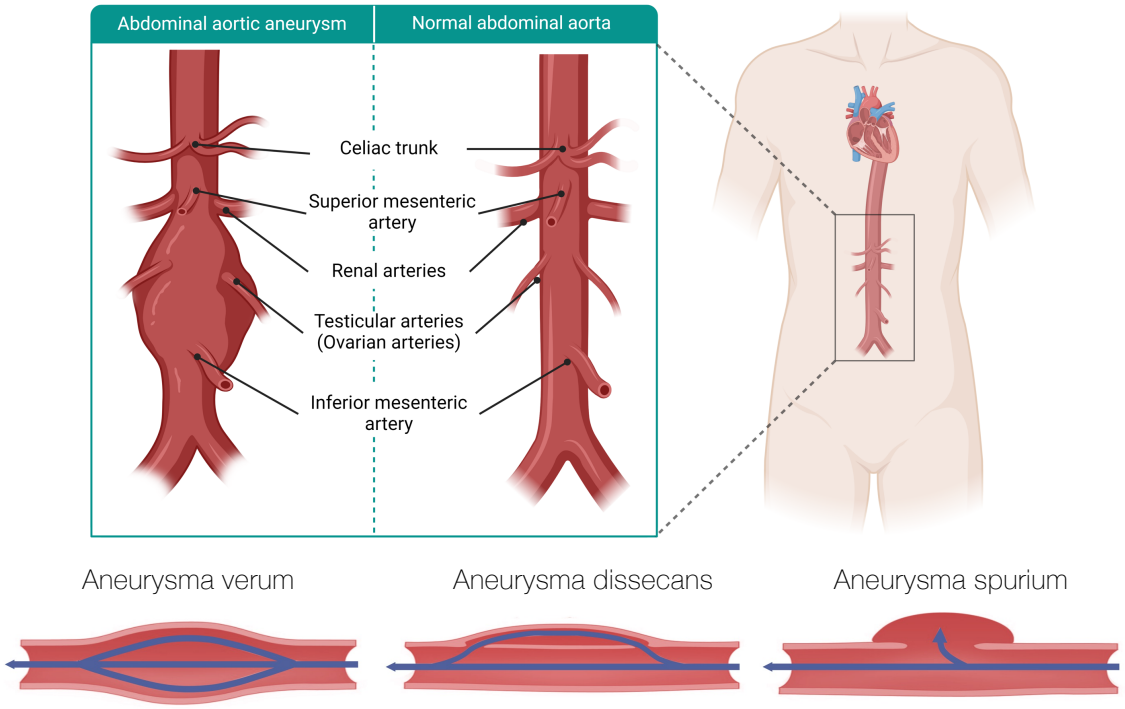

Fig. 5-1: The anatomy of the aorta and different types of AAAs

The illustration depicts the anatomy of the aorta and its various branching arteries. It also showcases different types of AAAs, each affecting different layers of the arterial wall. Based on the defect, distinctions are made between true aneurysm or *Aneurysma verum* (outpouching of all layers), dissecting aneurysm or *Aneurysma dissecans* (tear of the intima and splitting of the vascular wall with the formation of a second lumen), and false aneurysm or *Aneurysma spurium* (perforation of the vascular wall with the formation of an extravascular hematoma). Created with Biorender.com

5.2 Vascular Inflammation

Vascular inflammation is an adaptive and reactive process that can be triggered by chemical, biological or physico-mechanical irritations of the tissue (Chen et al., 2018). These stimuli are initiated by various extracellular mediators such as cytokines, NET formation, lipid-mediators and granule protein secretion, and small molecules such as adenosine triphosphate (ATP), which are released by stressed cells (Medzhitov, 2008, Feng et al., 2020). Such extracellular mediators lead to the activation, recruitment, and action of the humoral and cellular immune systems. These mediators not only affect the immune system but also structural tissues of the vessel, such as the endothelium, smooth muscle cells, and fibroblasts, enhancing their interaction with immune cells. For immune cells to enter the vessel wall, they need to undergo the well-known process of selectin-mediated rolling, activation triggered by chemokines, integrin-dependent adhesion, intraluminal crawling and trans- or paracellular migration. Endothelial cells furthermore express surface molecules such as Vascular cell adhesion molecule-1 (VCAM1), Intracellular adhesion molecule-1 (ICAM1) and Endothelial cell-selective adhesion molecule (ESAM) (Ley et al., 2007), while interactions between immune cells and endothelial cells loosen the endothelial contacts via mechanisms like VE-cadherin–α-catenin interaction, significantly impacting immune cell extravasation (Vestweber, 2012). All these processes and modifications to the vessel wall allow the entry of various immune cells to act against potential invaders, which essentially leads to inflammation. There is no doubt that the process of vascular inflammation is cardinal in fighting potential invaders, however the resultant effector molecules, such as reactive oxygen species (ROS) or metalloproteases, that form as a result, can turn out to be harmful to the surrounding tissue and therefore further aggravate existing frailty of the vessel wall and promote chronic diseases, such as atherosclerosis, deep venous thrombosis and dissections or AAA (Bäck et al., 2019, Sakalihasan et al., 2018).

5.3 Purinergic Signaling

As fundamental components of nucleic acids inside the cell, nucleotides and nucleosides play crucial roles in metabolism and signal transduction (Hess and Greenberg, 2012). Nucleic acids, ATP, nicotinamide adenine dinucleotide (NAD+), and cyclic adenosine monophosphate (cAMP) all contain adenosine (Ado). With its energy-dense phosphodiester bonds, ATP is recognized as a significant energy carrier. NAD+, a

coenzyme that participates as an electron acceptor in a number of cellular redox processes, is another nucleotide. As part of glycolysis or fatty acid oxidation, NAD+ is reduced to NADH, which then acts as an electron carrier in the respiratory chain. The formation of nucleotides and nucleosides outside of cells is also possible (Abbracchio et al., 2009, Junger, 2011, Burnstock, 2012), where they serve as signaling molecules in a variety of physiological processes. There are several channels, transporters, enzymes, and receptors that are part of the complex purinergic metabolism and signaling cascade. Both passive lytic processes and active non-lytic methods can be used to release the nucleotides ATP and NAD+. P2 receptors can be activated by extracellular nucleotides, which primarily starts pro-inflammatory signaling cascades. Additionally, membrane-bound ectoenzymes constantly degrade the nucleotides by converting ATP and NAD+ in a cascade to Ado. According to the receptor subtype, Ado exerts pro- or anti-inflammatory actions when it binds to P1 receptors. Ado can also be degraded by enzymes in the extracellular environment or transported back into the cell by transporters, where it can be put together into nucleotides.

5.3.1 Adenosine Triphosphate

As already mentioned, the initiation and progression of inflammatory reactions are orchestrated by extracellular mediators such as extracellular ATP and Ado. Extracellular ATP is released by damaged or stressed cells as a result of processes such as necrosis and acts as a proinflammatory danger-associated molecule, whereas extracellular Ado is primarily regarded as an anti-inflammatory molecule (Linden, 2006, Ernst et al., 2010). Interestingly, extracellular ATP is rapidly metabolized by cell surface-expressed ectoenzymes like CD39 into adenosine monophosphate (AMP) (Antonioli et al., 2013). Furthermore, extracellular NAD can be degraded to AMP via another ectoenzyme, CD38 (ADP-ribosylcyclase/cADPR-Hydrolase 1). Both pathways stop at the nucleotide AMP, making the 5'ecto-nucleotidase CD73 the bottleneck for the generation of the anti-inflammatory nucleoside Ado (Harvey et al., 2020).

5.3.2 Adenosine

The extracellular Ado has an anti-inflammatory effect and can bind to four different Ado receptors (A1R, A2aR, A2bR and A3R) found on the cell surface, which belong to the superfamily of G-protein-coupled receptors (Fredholm et al., 2001). The G-Protein

receptors are vastly expressed on many cell types and trigger different functions. For instance, the A1 receptor is mostly found in the brain, such as the hippocampus and spinal cord, but also broadly throughout the body (Ballesteros-Yáñez et al., 2018, Chen et al., 2013). In terms of immune response, activation of this receptor is pro-inflammatory due to the secretion of tumor necrosis factor-alpha (TNF-α) and the subsequent production of ROS (Cronstein et al., 1990). Additionally, the A3R has been shown to have cardioprotective effects on coronary arteries (Nishat et al., 2016, Tracey et al., 1998). One cardinal function of these G-protein-coupled receptors is the modulation of immune responses. Extracellular Ado can bind to the low-affinity A2bR and exert anti-inflammatory effects via reducing endothelial cell production of ICAM1 and E-selectin, as well as diminishing endothelial cell-cell contacts (Eckle et al., 2008, Yang et al., 2006). Furthermore, A2bR activation affects myeloid cells such as macrophages, where IFN-γ-induced MHC class II expression is downregulated (Xaus et al., 1999), and neutrophils, where oxidase function is inhibited (van der Hoeven et al., 2011). The interaction with the high-affinity A2aR causes the inhibition of TNF-α and IL-12 in macrophages (Haskó and Cronstein, 2013, Kreckler et al., 2006). Lymphoid cells, such as T-cells, are also affected, with the release of IL-12 from both $CD4^+$ and $CD8^+$ T-cells being inhibited. (Naganuma et al., 2006, Erdmann et al., 2005). Considering this evidence, it appears that the activation of Ado receptors plays a significant role in controlling inflammation within the vascular wall. Given that the natural half-life of Ado in blood is only a few seconds (Parker and McCollam, 1990) and that its ubiquitous presence could amplify negative effects, CD73 may serve as an attractive gatekeeper for pharmacological modifications of the extracellular purinergic system during inflammation.

5.3.3 CD73

The primary enzyme that changes extracellular AMP into Ado is CD73. Consequently, numerous studies utilizing $CD73^{-/-}$ mice have examined how CD73 affects inflammatory disorders (Eichin et al., 2021). It has been established that CD73 is essential for hypoxia-induced vascular leakage in the colon, lungs, heart, and kidneys, as well as for the promotion of organ dysfunction by edema in sepsis or ischemic disorders (Thompson et al., 2004, Haskó et al., 2011). In fact, there is mounting evidence that CD73 may modulate myocardial infarction, where T-cells in particular may be crucial

to the recovery process by inhibiting fibrosis, decreasing infarct size, and reducing proinflammatory cytokines like IL-6 (Eckle et al., 2007, Borg et al., 2017, Quast et al., 2017). Furthermore, CD73 appears to have an impact on other vascular disorders. Zernecke et al. demonstrated that CD73 offers protection against the development of neointima and vascular inflammation in a carotid wire injury model (Zernecke et al., 2006). Additionally, there is proof that CD73 deficiency in ApoE-deficient animals induces atherosclerosis (Buchheiser et al., 2011). But there are also contradictory findings. Sutton et al. were able to demonstrate that CD73's protective effect on atherosclerosis alters as mice age, as the effect of plaque buildup was seen to reverse in 32 to 52-week-old mice (Sutton et al., 2020).

5.4 Osmotic Minipumps

In order to initiate and provoke the formation of vascular inflammation, where an AAA could be inevitable, the blood pressure of the mice can be raised with the aid of osmotic minipumps filled with Ang II, which are subcutaneously implanted for a period of 10 days in our study. The infusion time is often 4 weeks or even longer when using the minipumps stated above, which is a widely used model (Xu et al., 2023, Yao et al., 2023, Wu et al., 2022). Osmotic minipumps are devices that release a drug or other material continuously over time, generally for several days to several weeks (Almoshari, 2022). They function by directing the flow of the material through a tiny tube or cannula using an osmotic pressure gradient (Theeuwes and Yum, 1976). Osmotic minipumps are frequently used in pharmacology, toxicology, and neuroscience research, among other areas of study. These pumps provide several benefits over conventional drug delivery techniques, including the capacity to transport medications to particular parts of the body and to provide a steady and regulated release of the medication (Davila, 1992). Animal research has made extensive use of osmotic minipumps as a device to deliver a precise and constant amount of a substance over an extended period of time. One of the very first studies, published in 1978, demonstrated the importance of the minipumps in experimental research, showing that animals utilized in the experiments would not be disturbed for frequent injections, while a steady-state distribution of the substance can be guaranteed (Struyker-Boudier and Smits, 1978). In a study, it was discovered that hypertension in rats could be induced using osmotic minipumps that were filled with Ang II. The hormone was continuously

released from the pump due to the consistent osmotic pressure brought on by the water inflow (Kuroki et al., 2014). Another study by Daugherty et al. showed the infusion of losartan, an antagonist of the ATI receptor, into hyperlipidemic mice (Daugherty et al., 2001), among numerous other studies, using a similar approach. Using osmotic minipumps to provide Ang II has several benefits over more conventional techniques of hormone administration, including the ability to deliver a steady and controlled hormone release (Sareen et al., 2012).

5.5 Angiotensin II

A key part of the renin-angiotensin-aldosterone system (RAAS), a linked endocrine system crucial for controlling blood pressure and volume, is the endocrine peptide hormone angiotensin (Ang) (Patel et al., 2024) . Ang II is a hormone essential for controlling the body's fluid balance and blood pressure (Fyhrquist et al., 1995). It is produced when the enzyme angiotensin-converting enzyme (ACE) reacts with the precursor hormone angiotensinogen. Ang II then acts on the Ang II receptor type 1 (AT1) and Ang II receptor type 2 (AT2) to cause vasoconstriction and the production of aldosterone, a hormone that controls the balance of salt and water in the body (Hattangady et al., 2012). With the use of an osmotic pump, an overdose can have pro-inflammatory effects and trigger immunological reactions in the vasculature (Ruiz-Ortega et al., 2002). According to one study, Ang II is crucial for the emergence of hypertension, a significant risk factor for cardiovascular disease (Welch, 2008). According to the study, Ang II causes vasoconstriction and an increase in blood pressure when it interacts with the AT1 receptor, and inhibiting this interaction can lower blood pressure in people with hypertension. Other research has shown the connection between Ang II and hypertension and revealed that treating hypertension by specifically targeting the RAAS can be successful (Krause et al., 2011, Williams et al., 2004).

5.1 Magnetic Resonance Imaging

The primary cornerstone of investigating the various segments relative to aortic anatomy and calculating the total area is magnetic resonance imaging (MRI), which stands out as a highly reliable method. Through the use of a gradient system, MRI permits three-dimensional spatial coding. Gradients can be turned on to slightly alter the

nuclei's excitation frequency, allowing three-dimensional images to be built from the energy emitted. Contrary to other imaging techniques like Single Photon Emission Computed Tomography (SPECT), Positron Emission Tomography (PET), or Computed Tomography (CT), MRI does not use ionizing radiation or a radioactive nucleus and is, thus, safer for patients (Ahrens and Bulte, 2013). It is now a standard method in regular clinical practice. MRI also allows for the application of various mapping techniques and spectroscopic investigations and provides great contrast between various tissues (Lee et al., 2014, Tirotta et al., 2015). However, with conventional methods, it can be challenging to discern specific tissue structures. In light of this, different contrast agents are usually needed (Burtea et al., 2008).

5.2 Ultrasound

Moreover, ultrasonography, a widely employed method, serves as a valuable tool for early screening to identify morphological or functional alterations in the aorta and played a pivotal role in the current study. Internal organs of the body can be imaged non-invasively and without exposure to ionizing radiation, using ultrasonic technology. High-frequency scanning can detect the velocity and flow of blood in arteries and veins (Anderson, 1995). When it comes to identifying AAA, ultrasound has a high specificity (almost 100%) and sensitivity (95%) (Keisler and Carter, 2015). Furthermore, ultrasonography is an inexpensive, safe, and widely utilized diagnostic tool for AAA (LeFevre, 2014, Schäberle et al., 2015). In 99% of individuals, ultrasound imaging can visualize the aorta (Lindholt et al., 1999). It has also been validated against reconstructed three-dimensional CT imaging of the aorta as being non-invasive, non-ionizing, and not requiring the use of nephrotoxic contrast agents (Meyenburg et al., 1990, Sprouse et al., 2004). In the last decade, advances in ultrasound imaging have made it possible to obtain accurate images of mouse (Steudel et al., 1998, Tanaka et al., 1996) and rat hearts (Burrell et al., 1996, Cittadini et al., 1996, Forman et al., 1997, Litwin et al., 1994), making it a reliable tool in rodent studies.

5.3 Flow Cytometry

Finally, a crucial aspect addressed in this study is the quantification of immune cells participating in the inflammation process, as well as the identification of various subgroups within these cells. Using fluorescence-coupled antibodies, fluorescence-

activated cell sorting (FACs) analyzes the cells' molecular and physical characteristics such as size, shape, surface markers, fluorescence and scattered light (McKinnon, 2018). The emission of photons from the fluorescent dye is activated when the tagged cells pass through a laser beam of an appropriate wavelength in a flow cytometer (Wilkerson, 2012). Light scattering and diffraction are influenced by cell shape and granularity (Adan et al., 2017). Flow cytometry is therefore an accurate measurement method for determining the number and activation status of immune cells in blood samples (Hoffman and Hansen, 1981). Understanding the immunological response to infection, illness, or immunization is crucial. Other studies have shown the value of flow cytometry in determining the level of immune cell activation in cancer patients, which can be used to forecast therapy response and track the development of the disease (Chanda et al., 2022, Blache et al., 2021). In cancer research, flow cytometry measured the expression of cell surface markers, which can be utilized to differentiate cancer cells from normal cells and identify them (Baran et al., 1998). This technique aids in the development and monitoring of cancer treatments as well as the discovery of novel cell surface markers linked to disease progression and progression-free survival.

6. Materials

6.1 Devices

Centrifuge	Beckman Coulter (Brea, USA)
Flow cytometer	BD Biosciences, FACSCanto™ II (San Jose, USA)
Gentle MACs Dissociator	Miltenyi Biotec (Bergisch Gladbach, Germany)
Incubator	Thermo Fisher (Rockford, USA)
Microscope	Olympus (Hamburg, Germany)
MR- Microimaging System	Bruker (Rheinstetten, Germany)
MR- Resonator Coil	Bruker (Rheinstetten, Germany)
MR- Spectrometer	Bruker (Rheinstetten, Germany)
Pipette Eppendorf (0,5-10, 10-100, 100-1000 µl)	Eppendorf (Hamburg, Germany)
Refrigerator -20°C	Liebherr (Kirchdorf, Germany)
Refrigerator -80°C	Thermo Fisher Scientific (Waltham, Massachusetts, USA)
Scotsman AF 80 Ice Flaker	Scotsman Ice (Milan, Italy)
Sterile Bench	Labogene (Lynge, Denmark)
Transducer (MX 550- Vevo 3100)	FUJIFILM, VisualSonics (Toronto, Canada)
Vortexer	VWR International (Darmstadt, Germany)

Table 6-1: Table 1 lists the various devices utilized in this study, along with their respective manufacturers.

6.2 Consumable Supplies

Eppendorf Tube (250 µl, 500 µl, 1,5 ml, 2 ml)	Greiner Bio One (Kremsmünster, Austria)
15 ml-Falcon	Greiner Bio One (Kremsmünster, Austria)
50 ml- Falcon	Greiner Bio One (Kremsmünster, Austria)
96-Well-Plate	Greiner Bio One (Kremsmünster, Austria)
C-Tube	Miltenyi Biotec (Bergisch Gladbach, Germany)
EASYstrainer (40 µm, 70 µm, 100 µm)	Greiner Bio One (Kremsmünster, Austria)
Eppendorf Safe Lock Tubes (1.5ml)	Eppendorf Quality (Hamburg, Germany)
Eppendorf Tube (250 µl, 500 µl, 1,5 ml, 2 ml)	Greiner Bio One (Kremsmünster, Austria)
Glass Tubes (25 ml, 50 ml, 100 ml, 250 ml, 500 ml)	Duran (Wertheim, Germany)
Isoflurane	Actavis GmbH (Langenfeld, Germany)
Nitrile glove 'Micro-Touch Nitra- Tex'	Ansell (Brussels, Belgium)
Osmotic Minipumps	Alzet, DURECT (Cupertino, USA)
Pipette Tips	StarLab (Hamburg, Germany)
Scalpel	Feather Safety Razor Co (Osaka, Japan)
Scissors	Paul Hartmann (Heidenheim, Germany)
Syringe	Becton Dickinson (Heidelberg, Germany)

Table 6-2: Table 2 lists the supplies consumed in this study, along with their respective manufacturers.

6.3 Chemicals

Depilatory Cream	Veet (Canada)
FcR Blocking Reagent	Miltenyi Biotec (Bergisch Gladbach, Germany)
Heparin	B. Braun AG (Melsungen, Germany)
MACs MicroBeads	Miltenyi Biotec (Bergisch Gladbach, Germany)
MACs Puffer	Miltenyi Biotec (Bergisch Gladbach, Germany)
PBS	Carl Roth (Karlsruhe, Germany)
RPMI 1640 Medium	Thermo Fisher Scientific (Waltham, Massachusetts, USA)
Tumor Dissociation Kit	Miltenyi Biotec (Bergisch Gladbach, Germany)
Ultrasonic Gel	Supragel (LCG, France)
FcR Blocking Reagent	Miltenyi Biotec (Bergisch Gladbach, Germany)

Table 6-3: Table 3 lists the different chemicals in this study, along with their respective manufacturers.

6.4 Antibodies

CD45	PerCP-Cy5-5	BD Biosciences
CD3	FITC-A	BD Biosciences
CD4	PECy-7	eBioscience
CD8	APC-H7	BD Biosciences

ENPP1	APC-A	BD Biosciences
CD38	APC-Cy7	BD Biosciences
CD39	AmCyan	BD Biosciences
CD73	AmCyan	Biolegend
F4/80	APC-A	BD Biosciences
Ly6G	PE-A	BD Biosciences
CD11b	FITC	Biolegend
DAPI	4′,6-Diamidin-2-phenylindol	Merck

Table 6-4: Table 4 lists the antibodies utilized in this study, along with their respective manufacturers.

7. Methods

7.1 Mouse Models

Animal tests were conducted in compliance with the national animal protection guidelines (Az: 81-02.04.2021.A401) and were authorized by the Landesamt für Natur-, Umwelt- und Verbraucherschutz (LANUV) Nordrhein-Westfalen. Male and female mice ($CD73^{-/-}$ and $CD73^{+/+}$; 3 and 6 months old) were utilized in this investigation. They were housed in the Heinrich Heine University's central animal facility in Düsseldorf, Germany, and were provided a standard chow diet along with tap water ad libitum. In the table below, an overview of the population utilized in this study, is summarized. A total of 96 mice were included, further divided based on their genetic backgrounds ($CD73^{-/-}$ 53; $CD73^{+/+}$ 43); and sex. The groups were also divided in both before-baseline (BL) and after (d10) Ang II treatment.

Mouse population							
96							
$CD73^{+/+}$				$CD73^{-/-}$			
43				53			
Male (M)		Female (F)		Male (M)		Female (F)	
19		24		28		25	
before treatment (BL)	after treatment (d10)	before treatment (BL)	after treatment (d10)	before treatment (BL)	after treatment (d10)	before treatment (BL)	after treatment (d10)
9	10	12	12	15	13	13	12

Table 7-1: The table demonstrates the population of the mice utilized in this study, grouped based on the genetic background, sex, before and after treatment with Ang II.

7.2 Implantation of Osmotic Minipumps

Ang II (6 µg/µl solution in NaCl) was injected into the pump body (Alzet, DURECT, Cupertino, USA), which was then placed in an Eppendorf Safe-lock tube (Eppendorf Quality, Hamburg, Germany) that had been filled with 0.9% NaCl and left overnight in a 37°C warming cabinet (Thermo Fisher, Rockford, USA). Mice were given 0.1 mg/kg of buprenorphine intraperitoneally 30 minutes prior to surgery. Before the pump was implanted subcutaneously in a minimally invasive procedure, 3% isoflurane (Actavis GmbH, Langenfeld, Germany) was administered to the mouse through a homemade nose mask. The back of the head was first shaved, followed by the preparation of a subcutaneous pocket with blunt scissors (Paul Hartmann, Heidenheim, Germany), the

insertion of the pump, and finally the suturing of the skin with a criss-cross suture (6-0 suture). This process takes 5-7 minutes per mouse. The pump was then left for a period of 10 days.

7.3 The Timelines

Principally, the mice were separated in 3 different groups concerning the timeline and treatment with Ang II (Figure 7-1). In the first group, female and male $CD73^{-/-}$ and $CD73^{+/+}$ mice were compared in all 3 aspects prior to Ang II treatment to determine if there are any disparities before treatment. In the second group, female and male mice were compared with each other regardless of their genetic background, both before and after treatment, in order to compare the effect of Ang II on the development of vascular inflammation in males and females. The goal of the final group was to compare the effect of sex after treatment with Ang II.

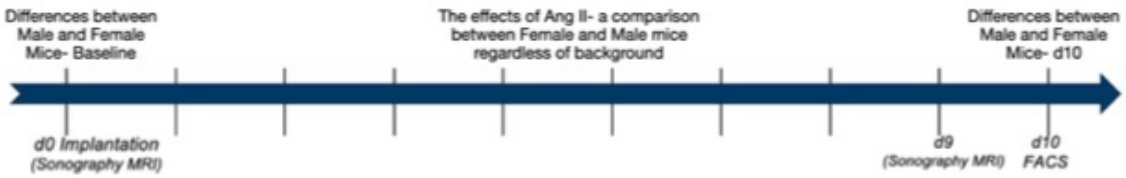

Fig. 7-1: Timeline for analyzing the mice

This began on d0 when morphological and functional aspects were assessed using the above-mentioned methods (Ultrasound and MRI). After this initial analysis, the mice were implanted with osmotic minipumps filled with Ang II and were left for 10 days (with a standard chow diet and tap water ad libitum). On d10 the same methods were used to analyze the differences between the female and male mice.

7.4 Immune Cell Isolation from the Aorta

The mice were given an intraperitoneal injection of 200 µl of a 0.2 molar heparine-PBS solution (B. Braun AG, Melsungen, Germany) 10 minutes before euthanization. Subsequently, the mice were euthanized after being anesthetized with 100 mg/kg ketamine and 10 mg/kg xylazine. The left common iliac artery was cut, the abdomen and thorax were opened, and the left ventricle was punctured with 20 ml of a PBS Solution (Carl Roth, Karlsruhe, Germany). The aorta was dissected, and all organs were removed. Nearly 1 mm below the aortic arch and 1 mm above the aortic bifurcation, the perivascular fat surrounding the aorta was carefully excised. Using the

tumor dissociation kit (Miltenyi Biotec, Bergisch Gladbach, Germany) and following the manufacturer's instructions, the immune cells from the recently removed aorta were separated using a gentle MACS dissociator (Miltenyi Biotec, Bergisch Gladbach, Germany). In summary, the aorta was digested over a period of 41 minutes using an enzyme mixture and RPMI (Thermo Fisher Scientific, Waltham, Massachusetts, USA) in a C-tube (Miltenyi Biotec, Bergisch Gladbach, Germany). Afterwards, cells were washed with MACS buffer, and debris were removed using a 40 µm cell filter.

Fig. 7-2: Comparison between Aortic Images from 2 Different Mice

Depicted are two examples of aortas prepared from 2 different mice. The aorta on the left was extracted with a normal diameter and washed free of any blood clots using a PBS Solution, while the one on the right shows an aneurysm with a blood clot, that couldn't be washed away with the solution, as a result of the treatment with Ang II.

7.5 Magnetic Resonance Imaging (MRI)

7.5.1 General

All experiments were conducted using a vertical 9.4 T Bruker AVANCE^{III} Wide Bore NMR spectrometer (Bruker, Rheinstetten, Germany) with a Bruker microimaging unit Micro 2.5 with actively shielded gradient sets (1.5 T/m) for ^{1}H measurements. A 25 mm ^{1}H resonator was used to collect the data. Mice were housed at 37 °C and anesthetized with 1.5% isoflurane (Actavis GmbH, Langenfeld, Germany). They were positioned inside the resonator to measure the abdominal aorta. A pneumatic pillow was used to

monitor the animals' respiration, and an M1025 system was employed to measure their vital functions (SA Instruments, Stony Brook, NY, USA).

7.5.2 Abdominal Aorta

Following axial pilot scans, the entire aorta was covered longitudinally across 36 sections, with 12 sections below and 24 sections above the lower renal vessel. The angio flash scan was conducted using the following parameters: ^{1}H fast low angle shot (flash); repetition time (TR) = 10.000 ms, FOV = 2.56×2.56 cm^2, matrix: 192×192, slice thickness (ST) 0.5 mm, and acquisition time (TAcq) 5 min.

7.5.3 Data Analysis

Internal software modules based on the LabVIEW package (National Instruments, Austin, TX, USA) were used to analyze MRI data, as proven to be reliable (Flögel et al., 2008, Ebner et al., 2010).

7.6 Ultrasound Scan

7.6.1 General

The mouse was placed on a thermostatically controlled heating pad in the supine position, sedated with 3% isoflurane (Actavis GmbH, Langenfeld, Germany), and its paws taped over the ECG electrodes attached to the table. A facemask attached to a coaxial circuit was used to give 1.8% isoflurane in 100% oxygen at a flow rate of 0.8 l/min to maintain anesthesia. ECG was used for respiratory gating. A depilatory cream (Veet, Canada) was applied to the abdomen using cotton-tipped applicators in a circular motion, and left for 30 seconds before being removed with a water-dipped gauze. A small-diameter temperature probe was then inserted through the anus. A colorless, aqueous, warmed ultrasonic gel (Supragel®, LCH, France) was applied between the skin and the transducer (MX 550- Vevo 3100 FUJIFILM, VisualSonics, Toronto, Canada) without air bubbles. The transducer was positioned on the abdomen with the heating pad inclined backwards by about 30 degrees. The aorta was located transversally in an epigastric angle using the transducer (40 MHz), then the transducer was rotated 90 degrees clockwise to locate the aorta sagittally. All measurements were

taken at the same position between the cranial mesenteric artery and the celiac artery. The mouse was then awakened from anesthesia under a heat lamp and observed after the ultrasonic gel and rectal probe were removed.

7.6.2 Strain

The values measured in M-Mode, where the layers of the aorta are presented and the systolic and diastolic diameters are assessed, can be used to determine the aortic strain, a measurement of vascular elasticity that indicates the stiffness of the aorta. The aorta must be crossed by the ultrasound waves perpendicularly. Aortic strain can be calculated using the following formula:

$$(½*[(Diameter_{systole}/Diameter_{diastole})^{2}-1]*100\%)$$

7.6.3 Blood Flow Velocity

Using the pulse wave mode, the peak systolic, end diastolic, and mean blood flow velocities can be calculated. On the screen, a measuring window, tilted at least 60 degrees toward the vascular path is visible. Fitted inside that window, the segment between the celiac trunk and the superior mesenteric artery was adjusted so that half to two thirds of the vessel diameter was examined. Once the blood flow velocity could be measured accurately, adjustments were made to the pulse repetition frequency and gain for optimal recording.

7.6.4 Data Analysis

Analysis was carried out using the Vevo LAB program to examine the imaging data.

7.7 Flow Cytometry

7.7.1 General

A FACS Canto II was used for the flow cytometry (BD Biosciences, USA). Proper forward/side scatter settings and thresholds were applied to exclude debris from the analysis. Samples were stained with 1 µg/ml DAPI (4′,6-Diamidin-2-phenylindol,

Merck) to omit dead cells. Depending on the experiment, cells were gated using the FACS Diva software, and either the mean fluorescence intensities or the quantity of positive cells were calculated.

7.7.2 Mouse Immune Cells

Antibody labeling was utilized to distinguish between various mouse immune cell types. FcR-blocking solution (Miltenyi Biotec, Bergisch Gladbach, Germany) was applied for 10 minutes at 4°C. After washing with 200 µl MACS buffer (Miltenyi Biotec, Bergisch Gladbach, Germany), staining against CD45 (BD Biosciences, clone 30-F11) and CD11b (Biolegend, clone M1/70) was conducted to label total immune cells ($CD45^+$), myeloid cells ($CD45^+$ + $CD11b^+$) and lymphoid cells ($CD45^+$ + $CD11b^-$), as well as CD73 (Biolegend, clone TY/11.8). After labeling for 20 minutes at 4°C, the cells were washed with 200 µl of MACS buffer.

7.7.3 Data Analysis

FlowJo_10.8.0 was used to examine data sets from flow cytometry.

8. Results

8.1 The Cardinal Aspects

The aim of this study was to observe the role of CD73 and its influenced gender-specific influence on the development of aortic dieseases following Ang II treatment, particularly during the early stages of vascular inflammation. Three critical aspects were assessed to compare the different populations: morphological, functional, and cytometric parameters. The morphological aspect, which is measured by means of magnetic resonance imaging to compare the anatomy and total area of the aorta in the cranio-caudal direction. The objective was to determine whether there were any differences induced following Ang II treatment (Figures 8-1A and 8-1D). The second parameter is the functional aspect of the aorta, which was evaluated via ultrasonography. This allowed for the visualization of the aorta and the measurement of blood velocity. Additionally, ultrasonography was used to assess the strain of the aortic walls, providing insight to the elasticity and stiffness of the aorta (Figure 8-1B and 8-1C). The final parameter is the cytometric aspect, which is measured using flow cytometry to quantify the number of immune cells infiltrating the aortic wall. The purpose was to determine if Ang II-induced vascular inflammation was occuring, which could precede the formation of an aneurysm. By examining these three aspects, we aimed to compare all the different populations separately to determine whether each factor (CD73 presence/absence, sex and Ang II treatment) played a role in promoting a vascular inflammation or even an AAA. As already mentioned above, different populations were utilized, which were further divided based on their genetic backgrounds ($CD73^{-/-}$ 53; $CD73^{+/+}$ 43); and sex (male 47; female 49). Osmotic minipumps were implanted subcutaneously in the mice for 10 days to investigate the effects of Ang II on the formation of vascular inflammation. All mice that had developed an AAA were excluded from the primary focus of our research, which was the early stages of aortic disease before significant structural changes formed. A pooling statistical approach was used to analyze the main effects of Ang II, sex and genetic background independently of the individual subgroups. This approach allowed us to maintain relatively low mouse numbers in accordance with the three Rs principle, ensuring ethical and efficient use of animal models in research.

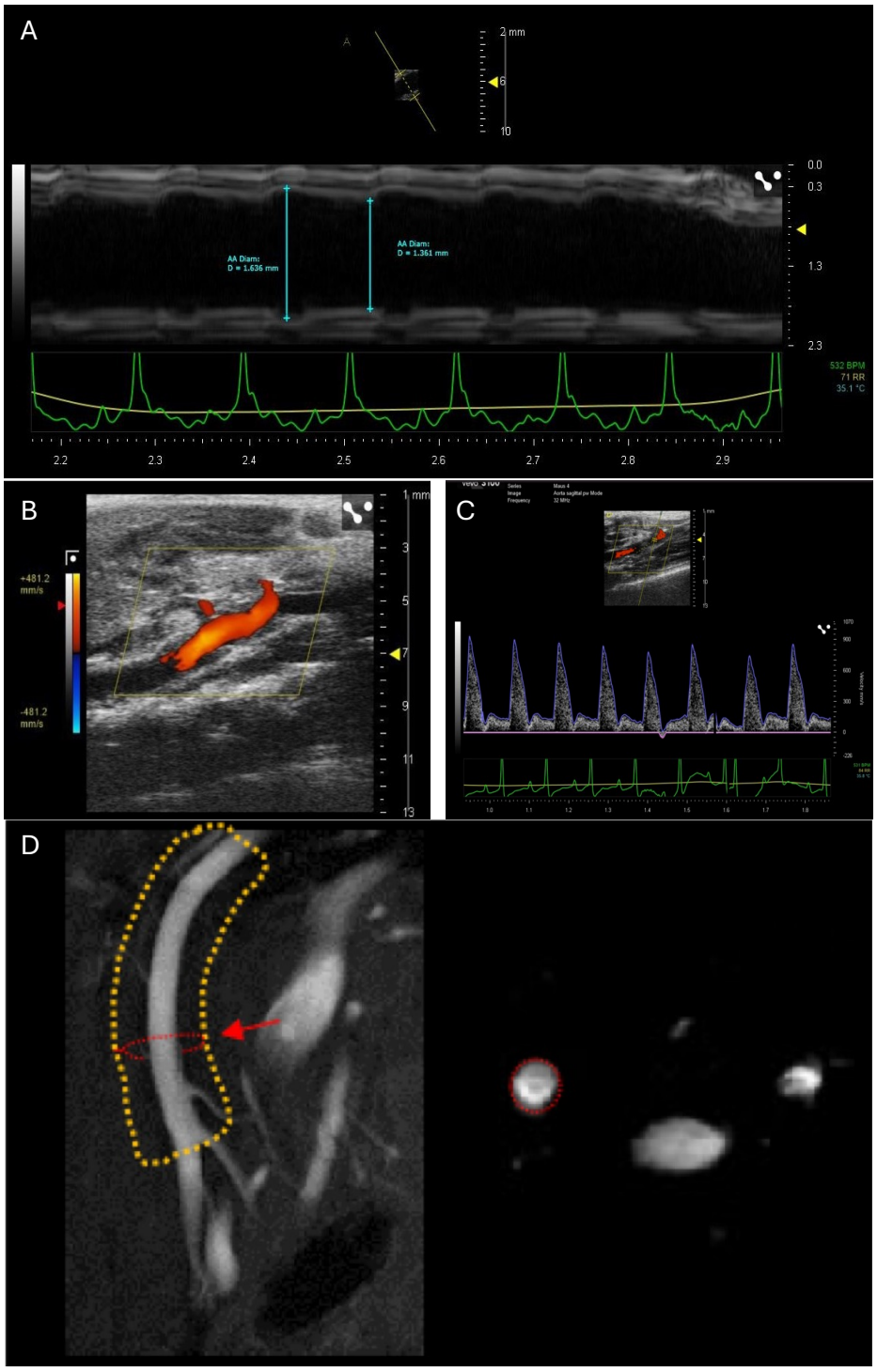

Fig. 8-1: Anatomical Visualization of the Aorta Using Ultrasound and MRI

A) The layers of the aortic wall are displayed in the M-Mode, where the systolic and diastolic diameters could be measured and with the help of a certain formula the strain can be deduced. B) Using the pulse wave mode, the peak systolic velocity and end diastolic velocity can be measured, from which the mean blood velocity can be deduced. The measurement window is tilted at least 60 degrees to the vascular path and positioned between the celiac trunk and the superior mesenteric artery. C) Using the color mode, the blood flow can be visualized. The superior mesenteric artery and the celiac trunk are displayed, providing a dynamic view of blood circulation. D) An overview of the abdominal aorta with the area of interest highlighted by an orange rectangle. This area was measured in the axial direction using FLASH angio

scans. An example of one section is highlighted by a red circle, with the corresponding transverse image displayed on the right. This imaging provides detailed information about the aortic anatomy and helps in identifying any structural changes induced by Ang II treatment.

8.2 Before Treatment with Ang II

As mentioned above, the mouse population was divided according to both the sex and genetic background and analyzed before the osmotic minipump implantation to determine if either model shows an increased pathological response. The mice were then assessed based on morphology via MRI, functionality via ultrasound, and finally the cytometric aspect using flow cytometry.

8.2.1 Morphological Aspect of Baseline Mice

For the morphological analysis, the aorta was scanned with the aid of a vertical 9.4 T Bruker AVANCE III Wide Bore NMR spectrometer in a longitudinal direction over the whole abdominal space. Using a 25 mm 1H resonator, data was gathered and 36 sections, with 12 sections below the lower kidney vessel and 24 sections above were analyzed. However, the quantification of the sectional areas of the aorta, which determined the vessel lumen, revealed no differences between $CD73^{-/-}$ and $CD73^{+/+}$ mice, as seen in Figure 8-2. It was clear, however, that the male mice had a larger lumen than the female mice, regardless of the genetic background. Additionally depicted in Figure 8-2 , the total area of the aorta was calculated and compared across all groups. This showed a statistically significant difference between the female and male groups, highlighting the anatomical differences in aortic size based on sex.

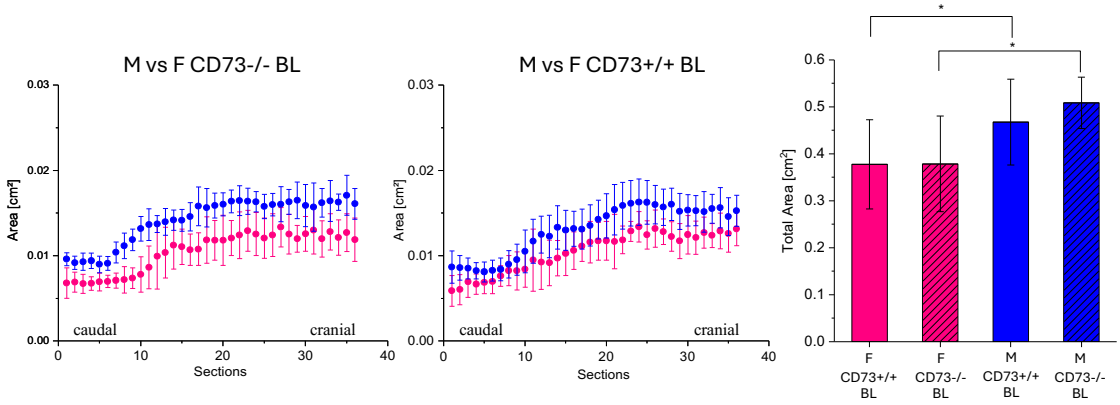

Fig. 8-2: Pre-Treatment MRI Analysis with Ang II

The vessel area was determined by axial flash scans via MRI. Quantification revealed that the male group (blue) had a larger lumen than the female group (pink), regardless of the genetic background. There was no noticeable difference between the $CD73^{-/-}$ and $CD73^{+/+}$ mice (solid= $CD73^{+/+}$, stripes= $CD73^{-/-}$). All datasets are mean values of individual experiments with the following group sizes: Male $CD73^{-/-}$ n = 8, Female $CD73^{-/-}$ n=8, Male $CD73^{+/+}$ n= 15, Female $CD73^{+/+}$ n=6. The total area of the aorta was compared across the four BL groups. Quantification showed that the genetic background does not significantly influence the total area. However, the female groups had a smaller total aortic area compared to their male counterparts, regardless of genetic background. This difference was statistically significant when comparing both the female and male groups, regardless of genetic background. All datasets are mean values of individual experiments with the following group sizes: Male $CD73^{-/-}$ n = 9, Female $CD73^{-/-}$ n=8, Male $CD73^{+/+}$ n= 15, Female $CD73^{+/+}$ n=6. Statistical significance was marked with *=P<0.05, by one-way ANOVA.

8.2.2 Functional Aspect of Baseline Mice

The MRI analysis yielded results that were not statistically significant, regarding the genetic background. Consequently, we investigated potential functional dissimilarities, focusing on alterations in vessel strain and blood flow velocity in both male and female mice, prior to the emergence of morphological disparities ($CD73^{-/-}$ and $CD73^{+/+}$), utilizing ultrasound imaging techniques. The results indicated no significant differences in functional aspects between the groups. However, the was a slight tendency for $CD73^{-/-}$ mice, both female and male, to exhibit lower strain compared to the $CD73^{+/+}$ mice, as illustrated in Figure 8-3. That change is not very noticeable in the mean velocity of the male group.

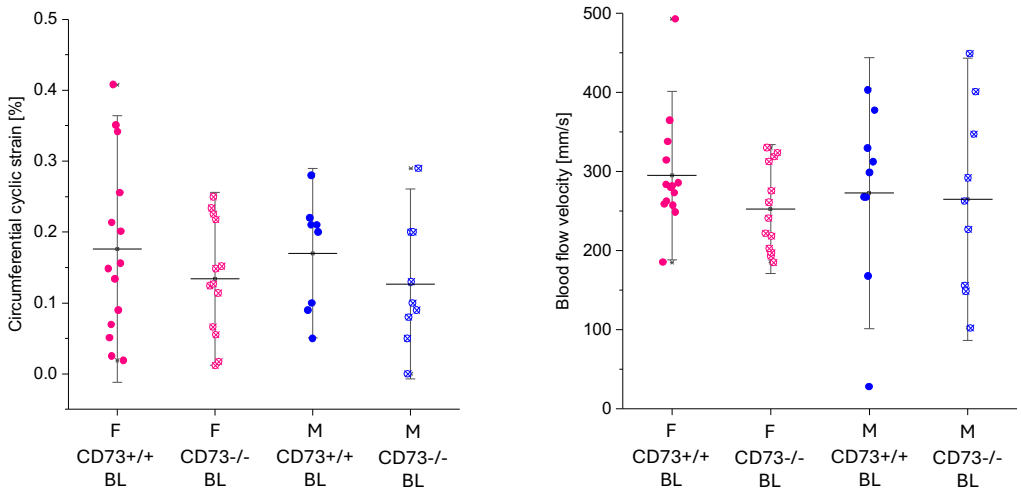

Fig. 8-3: Pre-treatment Ultrasound Analysis with Ang II

Vessel strain and blood flow velocity determined by ultrasound examination showed no significant differences between all groups. The $CD73^{-/-}$ groups showed less strain compared to $CD73^{+/+}$ mice before

Ang II treatment. However, differences regarding sex were not detectable. Almost the same can be noticed about the blood flow velocity. The $CD73^{-/-}$ group showed a slightly lower velocity compared to the the $CD73^{+/+}$ group, although that change is very insignificant within the male groups ($CD73^{-/-}$ and $CD73^{+/+}$). All datasets are mean values of individual experiments: Male $CD73^{-/-}$ n = 8, Female $CD73^{-/-}$ n=13, Male $CD73^{+/+}$ n= 9, Female $CD73^{+/+}$ n=14.

8.2.3 Cytometric Aspect of Baseline Mice

Following the ultrasound examination, which confirmed the absence of significant functional differences between the groups, we used flow cytometry to quantify the number and composition of immune cells ($CD45^{+}$) within the aortic vessel wall. This analysis aimed to understand the BL immune cell infiltration prior to Ang II exposure. Again, there was no significant difference between all the groups. The $CD73^{-/-}$ mice showed a tendency to have slightly more $CD45^{+}$ cells compared to $CD73^{+/+}$ mice. The same phenomenon is seen for the myeloid cells, however the male $CD73^{-/-}$ mice seem to have a slightly lower number of lymphoid cells compared to the male $CD73^{+/+}$ mice, as demonstrated in Figure 8-4. The male group showed fewer neutrophils compared to the female group, though this difference was not significant. The B-cells were almost the same across all groups and the T-cells were slightly higher in the male group compared to the female group. The macrophages were insignificantly higher in the $CD73^{-/-}$ mice irrespective of sex. These results indicate that there are no significant differences in the number of immune cells, including their subtypes, between the groups of female and male $CD73^{+/+}$ and $CD73^{-/-}$ mice before treatment with Ang II.

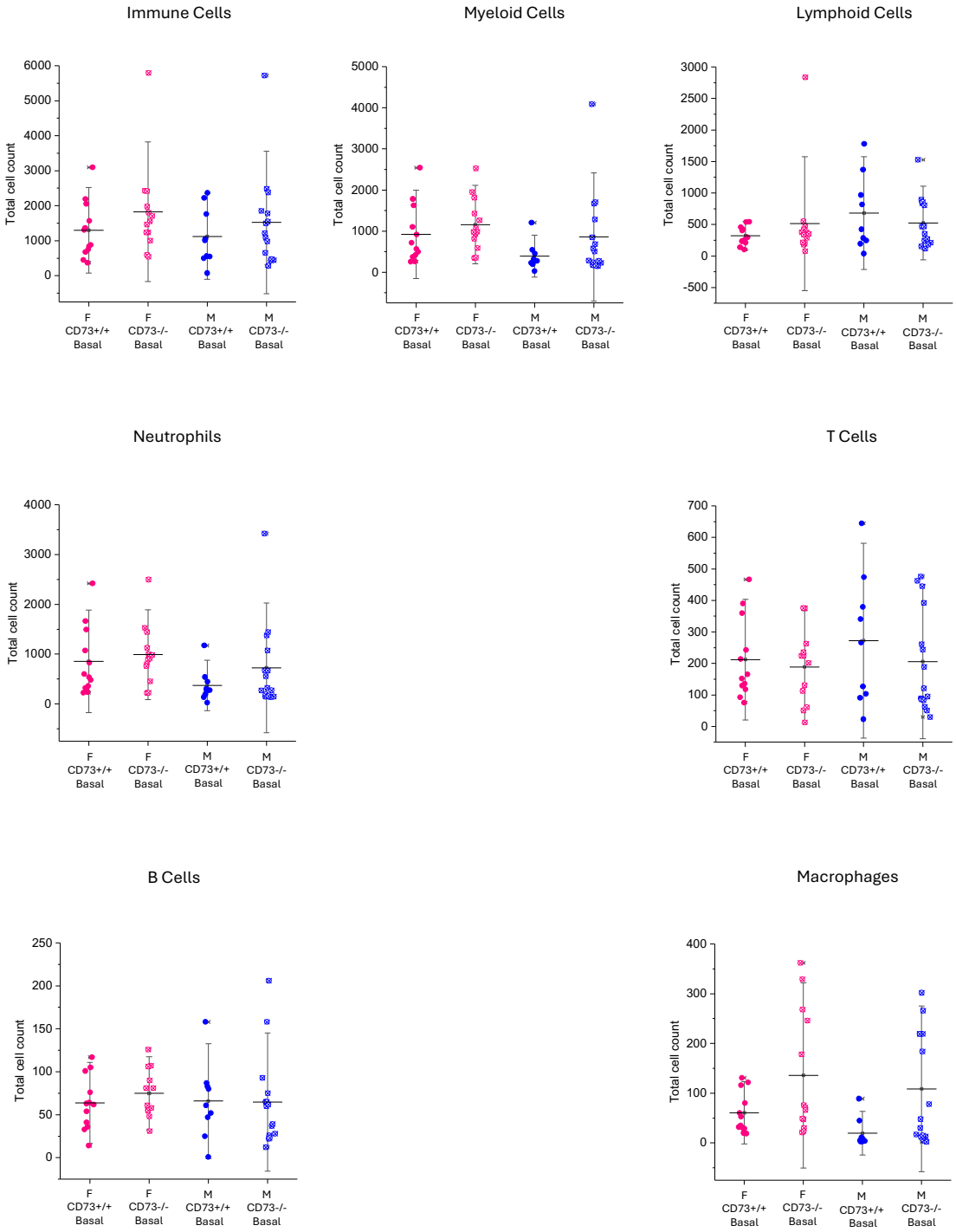

Fig. 8-4: FACs Analysis before Treatment with Ang II

Immune cells were isolated from the aortas of female (pink) and male (blue) $CD73^{+/+}$ (solid) and $CD73^{-/-}$ (cross) mice and counted via flow cytometry. Dead cells were excluded using DAPI staining. The total number of immune cells ($CD45^+$), myeloid cells ($CD45^+$ + $CD11b^+$), including macrophages ($CD45^+$ + $CD11b^+$ + $F4/80^+$) and neutrophils ($CD45^+$ + $CD11b^+$ + $Ly6G^+$), as well as lymphoid cells ($CD45^+$ + $CD11b^-$), including T-cells ($CD45^+$ + $CD11b^-$ + $CD3^+$) and B-cells ($CD45^+$ + $CD11b^-$ + $B220^+$), were quantified. We did not see any significant differences between total immune cells (A), the myeloid cells (B), lymphoid cells (C), neutrophils (D), B-Cells (E), T-Cells (F), or the macrophages (G). All datasets are mean values ± SD of n = 15-32 for each cell type (A-G).

8.3 The Effects of Ang II in Relation to Sex

The next phase is to compare whether the subcutaneously implanted osmotic minipumps filled with Ang II play a role in both male and female mice, regardless of their genetic background. This pooled approach allows for one variable to be held constant, enabling a clear determination of the effect of Ang II and proving this model as sustainable and reliable.

8.3.1 Morphological Aspect Baseline vs d10

The quantification of the sectional areas of the aorta was performed to determine the vessel lumen differences between the BL and d10 mice, regardless of their genetic backgound. As expected, an increase in the aortic lumen was observed in the female mice. However, in the male mice group, there was an intersection between sections 5 and 10 and around section 22, where the sectional lumen area of the d10 male mice was lower than the BL group, as displayed in Figure 8-5. The total area of the aorta was calculated and compared across all groups, also shown in Figure 8-5. There was a noticeable, significant difference between the BL and d10 female mice, with almost a 1.2x increase in the total area. Surprisingly, there was no significant difference between the BL and d10 male mice, indicating no observable effect of Ang II in the male group. The d10 male and female mice were very comparable, with almost the same total area.

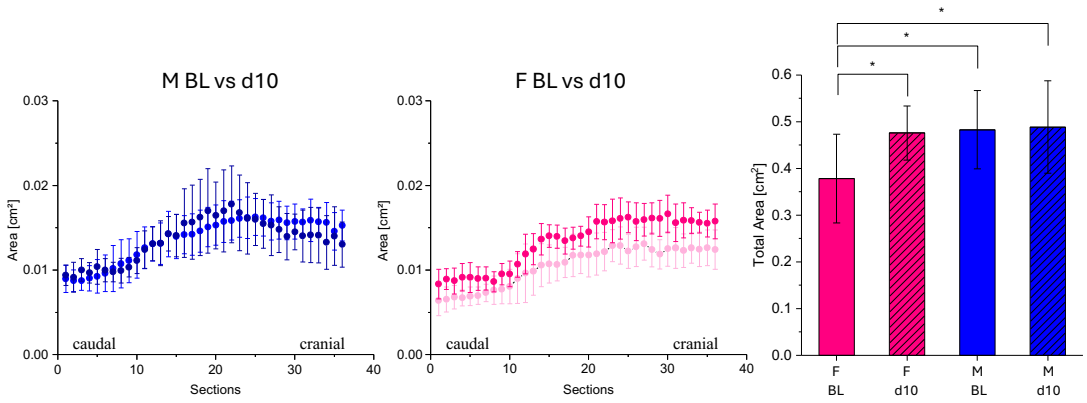

Fig. 8-5: Comparison of MRI Analysis Between Baseline and d10

Vessel area was determined by axial flash scans via MRI. Quantification revealed a higher lumen surface area in the d10 male and female mice compared to the BL group (light= BL, dark= d10). Notably, between sections 10 and 22, the lumen of the d10 male mice was larger than that of the BL mice. All datasets are mean values of individual experiments: Male BL n=24, Female BL n=14, Male d10 n= 7, Female d10 n=10. The total aortic area was determined and compared across all groups (solid= BL, stripes= d10). As anticipated, there was roughly a 1.2x increase in the overall area between the BL and d10 female mice, which was statistically significant. Surprisingly, there was no difference between the male mice in the BL and d10 groups, indicating that Ang II had no effect on the male group. The total area of the d10 male and female mice was nearly same, making them quite comparable. All datasets are mean values of individual experiments: Male BL n=24, Female BL n=14, Male D10 n= 7, Female D10 n=10. Statistical significance was marked with *=P<0.05, by one-way ANOVA.

8.3.2 Functional Aspect Baseline vs d10

The aortas were analyzed using ultrasound to compare the strain and velocity of the mice before and after Ang II treatment. The results showed no significant difference in strain between the female and male mice (BL vs. d10). However, the male d10 mice exhibited slightly higher strain compared to all groups, as displayed in Figure 8-6. A non-significant decrease in the mean velocity was observed in the female mice before and after Ang II treatment. In contrast, the male group showed a slight increase in velocity. Male mice exhibited almost twice the velocity compared to the female group, which is a statistically significant difference.

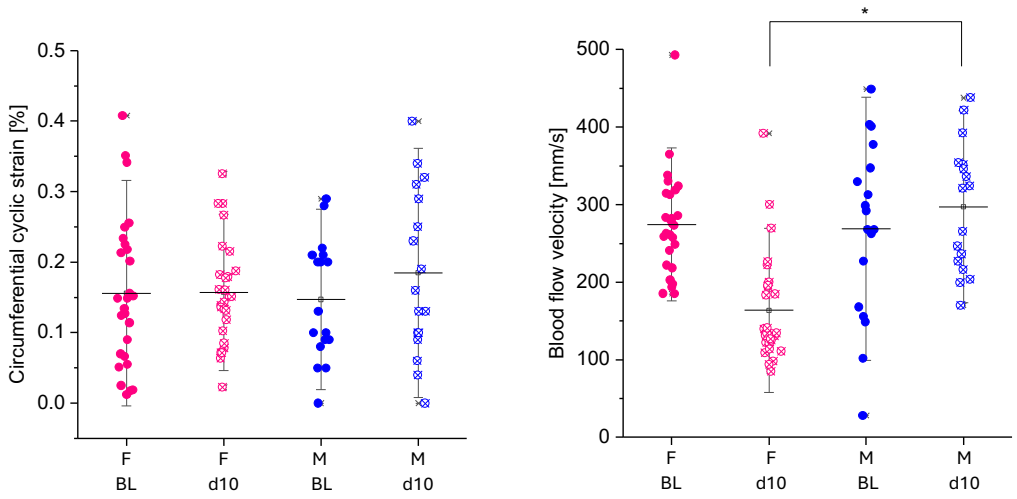

Fig. 8-6: Comparison of Ultrasound Analysis Between BL vs d10

Vessel strain showed no significant differences between all groups. However, there was a significant difference in blood flow velocity between the female and male groups after Ang II treatment. All groups were very similar regarding vessel strain, although the male group showed a slight tendency to have higher strain. There was a drop in blood flow velocity in the female group after Ang II treatment and a slight increase in the male group post-treatment. All datasets are mean values of individual experiments: Male $CD73^{-/-}$ n = 8, Female $CD73^{-/-}$ n=13, Male $CD73^{+/+}$ n= 9, Female $CD73^{+/+}$ n=14. Statistical significance was marked with *=P<0.05, by one-way ANOVA.

8.3.3 Cytometric Aspect Baseline vs d10

After analyzing the morphological and functional aspects of the aorta, the cytometrical analysis was conducted to confirm the effect of Ang II on the infiltration of immune cells into the aortic wall as a result of vascular inflammation. Noticeable differences were observed when comparing the BL and d10 mice. As shown in Figure 8-7, the number of $CD45^{+}$ cells, which represent total immune cells, nearly doubled in both female and male mice (significant difference), further demonstrating the effect of Ang II on the development of vascular inflammation. In the myeloid cell population, there was a slight increase in the female group and a more significant increase in the male group. Lymphoid cells also showed a significant increase in all groups, with notable differences between female and male mice. The number of neutrophils in the d10 male mice showed a threefold increase compared to the BL male mice (500 vs. 1500), while no significant increase was observed in the female group. Significant differences were also seen in the T and B-cell populations between the male groups and between the female d10 and male d10 groups regarding B-cells. Although macrophages did not

show any significant changes, a deviation was observed in the male d10 group. These findings reinforce the impact of Ang II on immune cell infiltration and vascular inflammation, with distinct patterns observed across different immune cell types and between sexes.

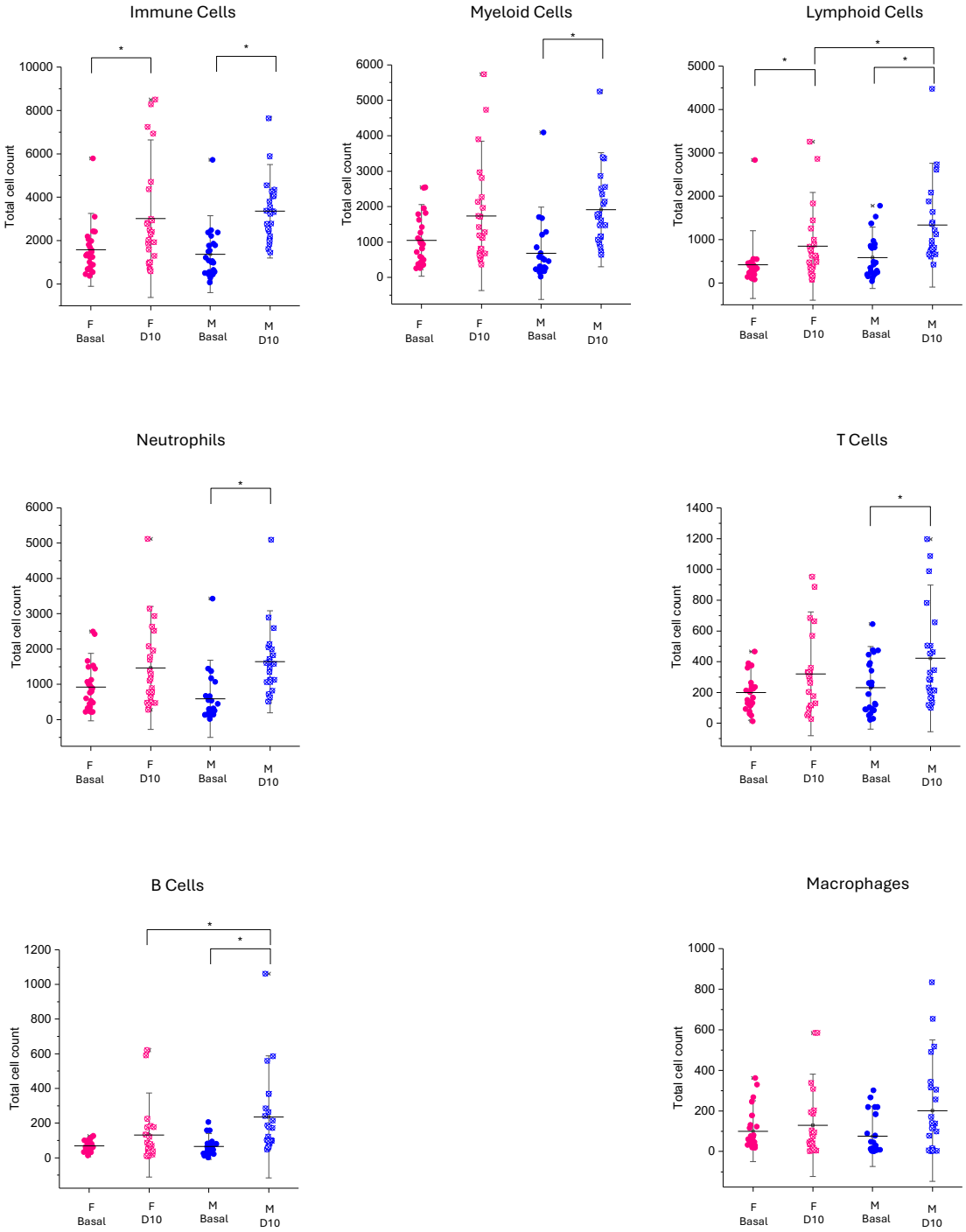

Fig. 8-7: Comparison of FACs Analysis Between BL vs d10

Immune cells were isolated from the aorta from female (pink) and male (blue) BL and d10 mice and counted via flow cytometry. Dead cells were excluded using DAPI staining. The total number of immune cells ($CD45^+$), myeloid cells ($CD45^+$ + $CD11b^+$), including macrophages ($CD45^+$ + $CD11b^+$ + $F4/80^+$) and neutrophils ($CD45^+$ + $CD11b^+$ + $Ly6G^+$), as well as lymphoid cells ($CD45^+$ + $CD11b^-$), including T-cells ($CD45^+$ + $CD11b^-$ + $CD3^+$) and B-cells ($CD45^+$ + $CD11b^-$ + $B220^+$), were quantified. The 10-day treatment with Ang II led to a significant increase in total immune cells, which is also visible in myeloid and lymphoid cells as well as neutrophils, T-cells and B-cells. All datasets are mean values ± SD of n = 15-32 for each cell type (A-G). Statistical significance was marked with *=P<0.05, by one-way ANOVA.

8.4 After Treatment with Ang II

The final phase of the study involved observing and comparing the groups after treatment with Ang II to determine if genetic background and sex influence the formation of vascular inflammation. The same pooling approach described perviously was utilized.

8.4.1 Morphological Aspect After Treatment with Ang II

The analysis of this group began with the measurement of the sectional areas of the aorta using MRI to determine the vessel lumen. Quantification revealed similar lumen sizes within the $CD73^{-/-}$ mice. However, it was evident that $CD73^{+/+}$male mice had a larger, though not statistically significant, lumen from section 15 to 27 compared to female mice, as shown in Figure 8-8. The total area of the aorta was compared across all groups. The $CD73^{+/+}$ groups, regardless of sex, showed a slightly higher total area than the $CD73^{-/-}$ mice. Additionally, the $CD73^{+/+}$ mice, had very similar total areas; the same observation applied to the $CD73^{-/-}$ mice. These findings suggest that while there are some variations in lumen size between male and female mice, the overall genetic background does not significantly impact the morphological aspects of the aorta following Ang II treatment.

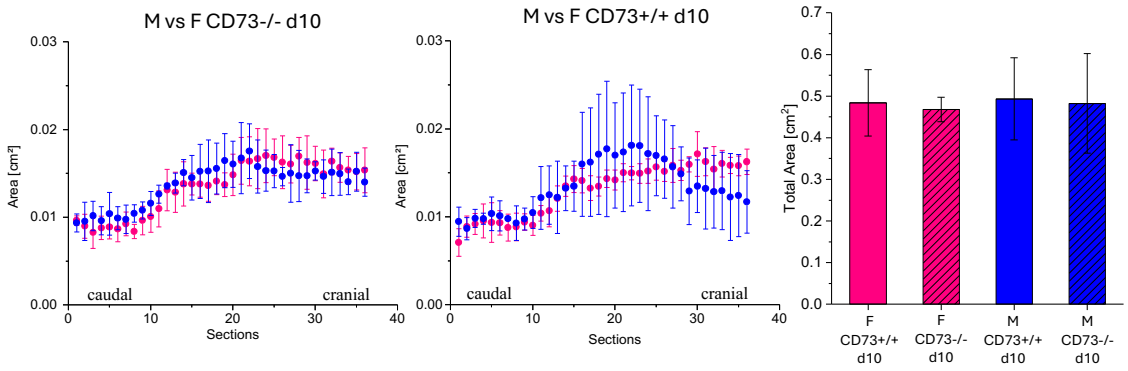

Fig. 8-8: MRI Analysis Post Treatment with Ang II

Vessel area was determined by axial flash scans via MRI. Quantification revealed that the male group (blue) had a larger lumen from section 15 to 27 compared to the female group (pink). However, cranially from section 30, the female $CD73^{+/+}$ group had a larger lumen. No significant differences were observed between the $CD73^{-/-}$ mice groups. All datasets are mean values of individual experiments: Male $CD73^{-/-}$ n=5, Female $CD73^{-/-}$ n=5, Male $CD73^{+/+}$ n= 4, Female $CD73^{+/+}$ n=5. The total aortic area was determined and compared across all groups, with no statistically significant differences observed (solid= $CD73^{+/+}$, stripes= $CD73^{-/-}$). The total area amounted to almost $0.5cm^2$. All datasets are mean values of individual experiments: Male $CD73^{-/-}$ n = 5, Female $CD73^{-/-}$ n=5, Male $CD73^{+/+}$ n= 4, Female $CD73^{+/+}$ n=5.

8.4.2 Functional Aspect After Treatment with Ang II

After Ang II treatment, it is important to observe any changes in blood flow dynamics and their effects on the aorta, as depicted in Figure 8-9. The results indicate a decrease in strain between the female $CD73^{-/-}$ and the $CD73^{+/+}$ mice. Conversly, both male groups showed an increase in strain. Both $CD73^{-/-}$ groups showed a decrease in mean velocity, although this was not statistically siginificant. Notably, the male $CD73^{-/-}$ mice demonstrated almost twice the velocity of the females, and the male $CD73^{+/+}$ mice had almost 1.5 times the velocity of the female mice. These findings suggest that Ang II treatment affects the functional dynamics of the aorta differently in male and female mice, with notable differences in strain and velocity between the sexes and genetic backgrounds.

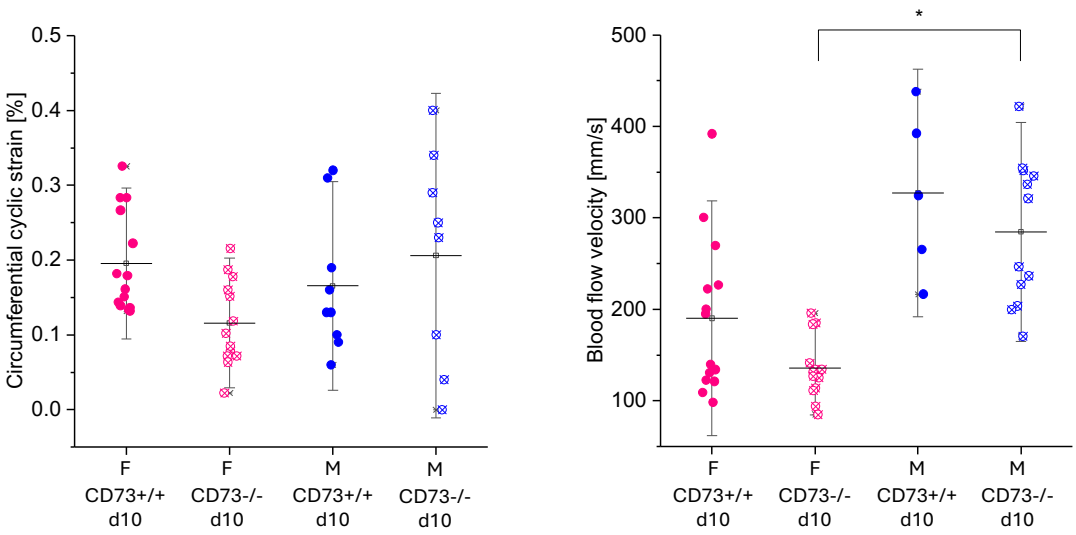

Fig. 8-9: Ultrasound Analysis Post Treatment with Ang II

Vessel strain determined by ultrasound examination showed no significant differences between all groups. The female $CD73^{-/-}$ group showed the lowest velocity among all groups and lower compared to the $CD73^{+/+}$ female group. The male $CD73^{-/-}$ group showed a higher velocity than the male $CD73^{+/+}$ group and the highest among all groups. Regarding velocity, the female $CD73^{-/-}$ group showed the lowest velocity, while the male group regardless of genetic background, exhibited higher velocities. However, there was a decrease in the velocity in the $CD73^{-/-}$ mice in both male and female groups. All datasets are mean values of individual experiments: Male $CD73^{-/-}$ n = 12, Female $CD73^{-/-}$ n=13, Male $CD73^{+/+}$ n= 5, Female $CD73^{+/+}$ n=14. Statistical significance was marked with *=$P<0.05$, by one-way ANOVA.

8.4.3 Cytometric Aspect After Treatment with Ang II

The final phase involved examining the effect of Ang II treatment on immune cell infiltration in the aorta. The expectation was that different genetic backgrounds would lead to significant differences. Surprisingly, there was no noticeable difference in total immune cell numbers between all groups (Figure 8-10). Both female $CD73^{+/+}$ and $CD73^{-/-}$ groups showed similar total immune cell counts (around 3000), whereas the male groups, $CD73^{+/+}$ and $CD73^{-/-}$, had slightly higher counts, approximately 4000 and 3500, respectively. This outcome was unexpected, as CD73 normally leads to the production of the anti-inflammatory molecule Ado, and its absence would theoretically result in a more pro-inflammatory state due to the accumulation of AMP.

Examining the specific immune cell types revealed slight fluctuations. The male groups consistently showed slightly higher immune cell numbers compared to the female groups. There was a tendency for $CD73^{-/-}$ mice to have lower myeloid and neutrophil cell counts than $CD73^{+/+}$ mice, regardless of sex. The T-cell counts were similar

between the two genetic backgrounds. The male mice, regardless of the genetic background, showed a higher B-cell count than the female mice, however the genetic background had no significant effect. Macrophages were slightly higher in the CD73$^{-/-}$ groups, regardless of sex.

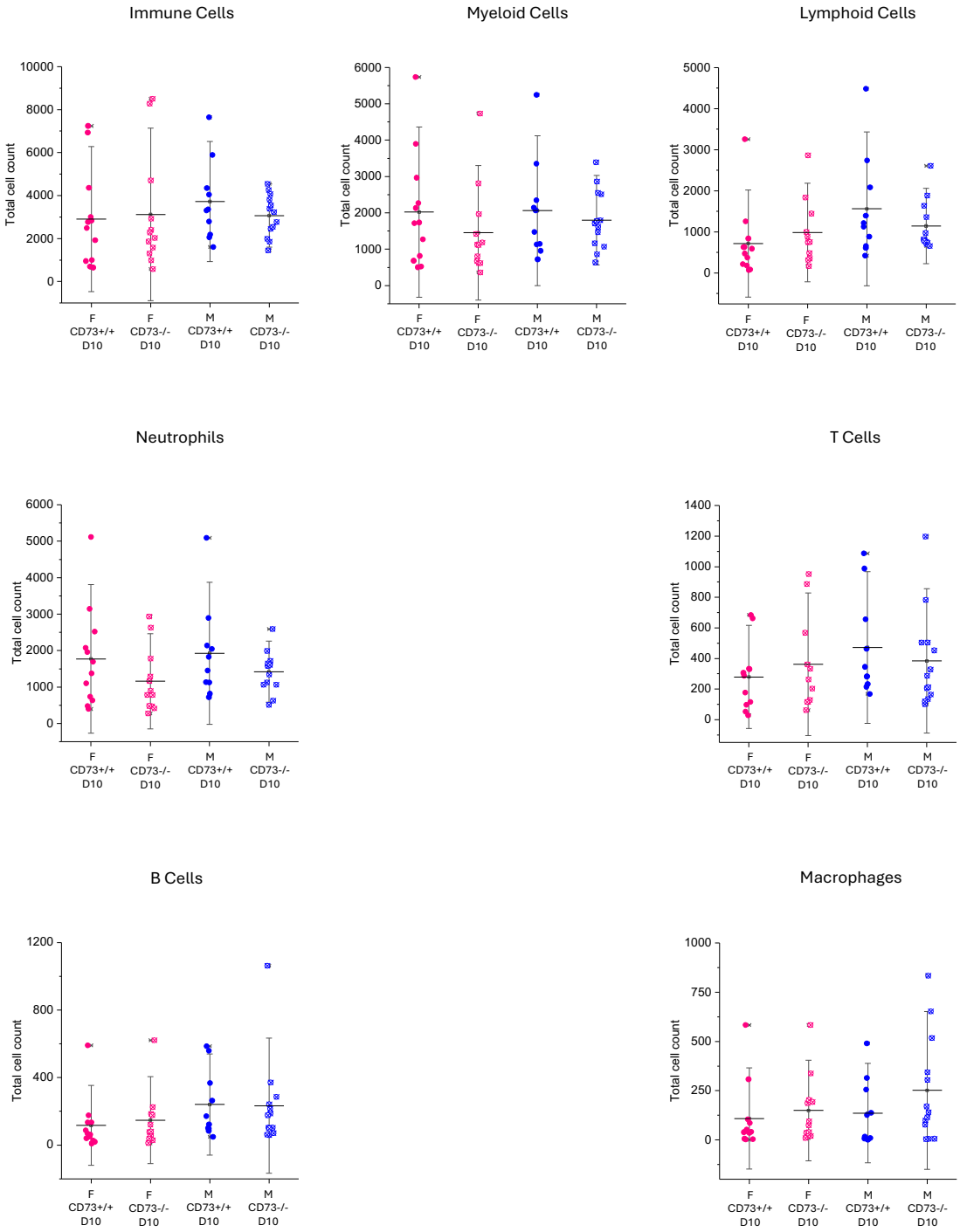

Fig. 8-10: FACs Analysis Post Treatment with Ang II

Immune cells were isolated from the aorta of female (pink) and male (blue) BL and d10 mice and counted via flow cytometry. Dead cells were excluded using DAPI staining. The total number of immune cells ($CD45^+$), myeloid cells ($CD45^+$ + $CD11b^+$), including macrophages ($CD45^+$ + $CD11b^+$ + $F4/80^+$) and neutrophils ($CD45^+$ + $CD11b^+$ + $Ly6G^+$), as well as lymphoid cells ($CD45^+$ + $CD11b^-$), including T-cells ($CD45^+$ + $CD11b^-$ + $CD3^+$) and B-cells ($CD45^+$ + $CD11b^-$ + $B220^+$), were quantified. No significant differences were observed in total immune cells (A), the myeloid cells (B), lymphoid cells (C), neutrophils (D), B-cells (E), T-cells (F), or the macrophages (G). All datasets are mean values ± SD of n = 15-32 for each cell type (A-G).

8.5 The Expression of CD73 is Reduced on Vessel-Infiltrating Immune Cells as a Result of Angiotensin II Treatment

In examining the relationship between CD73, an enzyme that degrades AMP into Ado, and cardiovascular diseases we investigated its role in early vascular inflammation within our present model. Using data from $CD73^{+/+}$ mice, we assessed the surface expression of CD73 on various immune cells, including myeloid and lymphoid cells. Our findings, depicted in Figure 8-11, reveal a threefold decrease in CD73 expression on total immune cells in both male and female mice following Ang II treatment. Myeloid cells showed a reduction in CD73 expression by a factor of five in females and 1.5 in males. Lymphoid cells exhibited a 2.5-fold decrease in CD73 surface expression in both sexes. Furthermore, neutrophils isolated from the aorta displayed a downregulation of CD73 following Ang II treatment, more pronounced in females than in males. However, T and B-cells maintained their CD73 expression patterns regardless of Ang II treatment. Macrophages, which infiltrate the aortic wall, showed the highest CD73 expression in the female $CD73^{+/+}$ group before treatment, approximately four times higher than the same group after treament. In contrast, the male groups showed a slight, barely noticeable increase in CD73 expression following Ang II treatment.

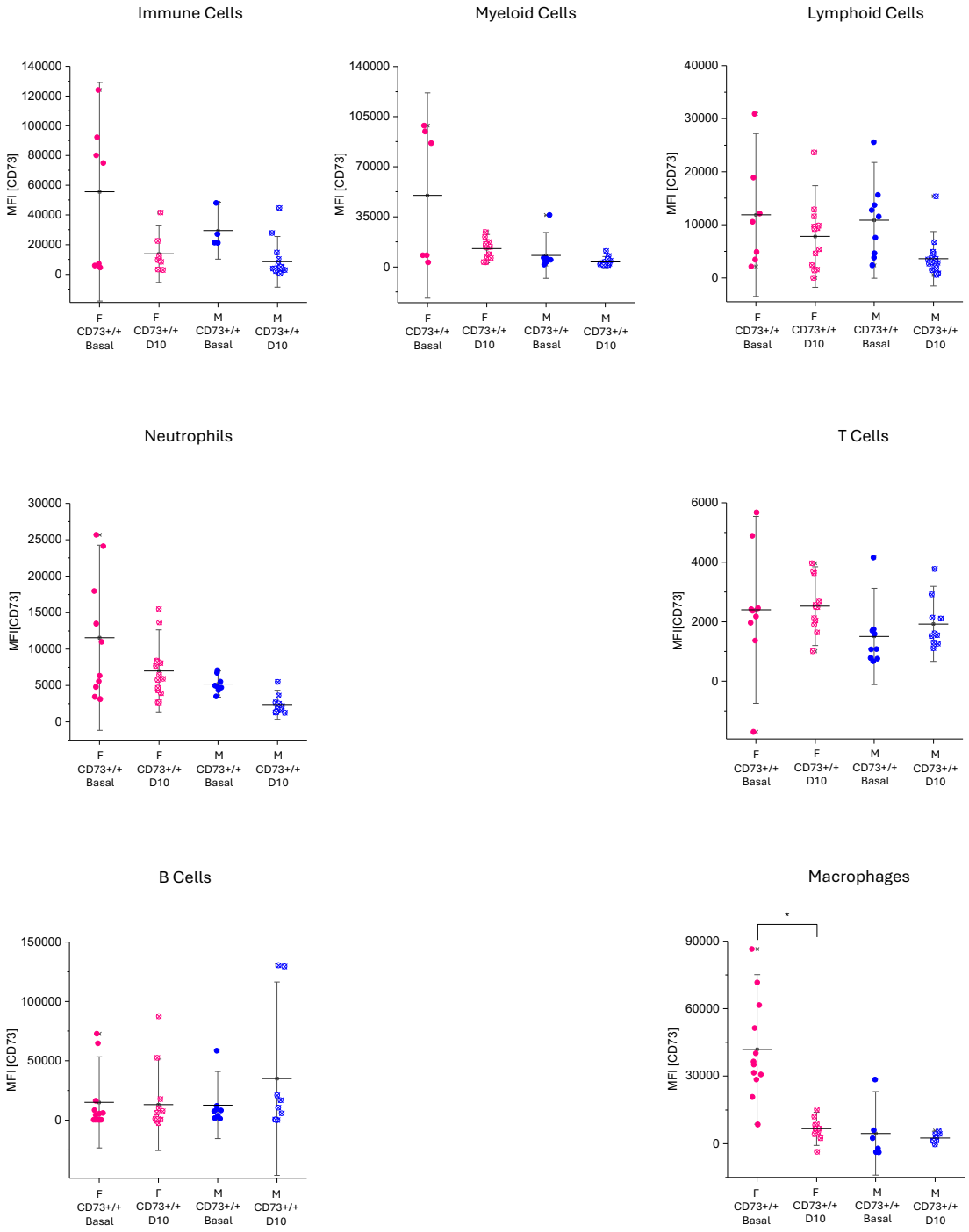

Fig. 8-11: Inflammation-Dependent Downregulation of CD73

The surface expression of CD73 was determined on total immune cells as well as specific immune cell subsets isolated from the aorta of $CD73^{+/+}$ mice under BL conditions (solid pink= females and solid blue= males) and 10 days after Ang II treatment (pink with a cross= females and blue with a cross= males) via flow cytometry. The analysis revealed a decrease in CD73 expression on total immune cells, myeloid, lymphoid cells and neutrophils after 10 days of Ang II treatment. All datasets are mean values ± SD of n = 16-23 for each cell type analyzed (A-G). Statistical significance was marked with *=P<0.05, by one-way ANOVA.

9. Discussion

In this study, we have demonstrated that mice, when treated with Ang II for a short period of 10 days via an osmotic pump, exhibit mild inflammation in the aorta without affecting the size of the blood vessel or its ability to withstand strain, even in the absence of ApoE deficiency or a high-fat diet. The same phenomenon has been shown in another study, which showed that Ang II induces inflammation without altering the blood pressure, highlighting the reliability of this model for studying early cardiovascular inflammation (de Lima et al., 2019). We were also able to show, that there was not a significant difference between male and female mice, in most parameters, except for the cytometric aspect, in regard to the treatment before and after Ang II. This makes the model suitable for studying the early processes involved in aortic diseases, specifically the initial stages of AAA formation.

Ang II is a vasoactive hormone that is a component of the RAAS, which controls electrolyte and fluid balance and is a target for current antihypertension treatments. It functions in a wide range of organs through AT1 and AT2 receptors, influencing blood pressure and sodium levels (Sparks et al., 2014). Additionally, Ang II can boost immune system activity and alter the vessel wall. For instance, Ang II stimulates splenic lymphocyte proliferation through the AT1 receptor through a calcineurin-dependent route and mobilizes splenic macrophages to promote aortic aneurysm formation (Nataraj et al., 1999, Mellak et al., 2015). It also stimulates an inflammatory response in the vascular wall by acting on endothelial cells, smooth muscle cells, monocytes, and lymphocytes (Berk et al., 2000).

Monocyte chemoattractant protein-1 (MCP-1), which is produced by endothelial and smooth muscle cells and whose expression is stimulated by Ang II, most likely mediates and amplify the effects of Ang II. It appears that Ang II enhances inflammation and accelerates atherosclerosis by boosting MCP-1 production, as deficiency of the main MCP-1 receptor (CCR2) lowers atherosclerosis in apoE$^{-/-}$ mice (Boring et al., 1998). Ang II is also known to activate NF-κB-dependent gene expression to stimulate VCAM-1 expression, and it is said to induce MCP-1 expression by a similar mechanism (Tummala et al., 1999). Additionally, Ang II increases the formation of ROS by activating vascular NADH oxidase (Griendling et al., 1994). This action may be due to

Ang II's particular effects on the expression or activity of MOX1, a subunit of the vascular smooth muscle cell NADH oxidase (Suh et al., 1999). In rodent studies, Ang II greatly increases the induction of vascular ROS compared to other vasoconstrictors such norepinephrine (Rajagopalan et al., 1996). As a result, it could be deduced that Ang II causes atherosclerosis through two different redox mechanisms: firstly, by raising the levels of lipid-oxidizing ROS, which encourages the loading of lipids into foam cells, and secondly, by promoting the production of redox-sensitive gene products, such VCAM-1 and MCP-1.

As already mentioned, the groups were split into different subgroups, which made the statistical analysis efficient and aligned with the 3 Rs regarding the number of mice included in this study. We started by measuring and analyzing the morphology of the aorta using MRI to establish BL values of the aortic diameter as a benchmark before treatment with Ang II and to check for sex-related differences. MRI does not require radiation and has been used in various studies also evaluate AAAs in mice (Bersi et al., 2020, Brangsch et al., 2019). In addition, time-of-flight angiography and black-blood spin-echo sequences can evaluate aortic morphology without contrast enhancement (Klink et al., 2011, Turner et al., 2008).

In the BL group, no significant differences were detected when comparing the different backgrounds of the male and female groups independently. However, the male groups generally demonstrated a higher aortic area, as assesed via MRI quantification, than females. This is expected since the male population generally exhibits a larger anatomy compared to females, as demonstrated in previous studies where the normal abdominal aortic diameter was analyzed and compared in the general population (Pham et al., 2019, Rogers et al., 2013, Hu et al., 2022, Wazzan et al., 2022).

To further assess the function of the aorta, mean blood velocity and aortic strain were also measured using ultrasound before administering Ang II to the mice. Ultrasound has been the method of choice for aneurysm screening and surveillance due to low cost, lack of exposure to radiation, and avoidance of nephrotoxic contrast agents. Additionally, it is noticeably quicker and more efficient compared to MRI (Lederle et al., 1997, Lindholt et al., 1999, Tayal et al., 2003, Lederle et al., 1988). Ultrasound reliably, effectively, and correctly identifies the existence of an AAA in asymptomatic individuals (Costantino et al., 2005, Rubano et al., 2013). Sensitivity and specificity are

close to 100%; however, in 1% to 3% of patients, intestinal gas or obesity prevents visualization of the aorta (Quill et al., 1989, Graeve et al., 1982). According to Wilmink et al., transabdominal ultrasonography has been proven to be one of the best methods for monitoring and screening (Wilmink et al., 2002). This way, any functional change in the aorta can be easily detected in the mice. The functional screening, however, showed no significant differences across all groups regarding sex and genetic background.

To continue the screening of the mice groups before treatment with Ang II and obtain a BL measurement for comparison, the aortas of the mice were prepared and measured for the number of immune cells found in the aortic wall. The different subpopulations were located and measured within a sample using flow cytometry. This method is very useful for analyzing the immunological makeup of mice aortas and has become increasingly popular over the past years. Additionally, flow cytometry can detect specific cell functional traits like proliferation, apoptosis, and cytokine production. It has also been used to measure immune responses in other organs and tissues such as the kidneys, heart and skin (Afanasyeva et al., 2004, Hammond, 1992, Wu et al., 2003).

In several studies, researchers have attempted to examine the aorta using flow cytometry, but the analysis has proven difficult due to residual tissue debris and cell loss during aorta preparation (Mattsson et al., 1991, Bonanno et al., 2000, Liu-Wu et al., 1997). In 2006, a flow cytometry-based technique was developed to examine aortic leukocytes using a combination of several enzymes (Galkina et al., 2006) . The quality of samples was greatly enhanced by including CD45, a common leukocyte marker, allowing for the exclusion of highly autofluorescent non-CD45 vascular cells from leukocyte analysis. Since then, other modifications to this approach and various enzyme combinations have been suggested for use in flow cytometry analysis (Butcher et al., 2011, Weber et al., 2011, Koltsova et al., 2012, Smith et al., 2010), which we adopted in our study to obtain the best possible results. Again, no significant difference was seen between all groups regarding sex and genetic background.

The next subgroup aimed to compare the effects of Ang II infusion via subcutaneously implanted osmotic minipumps. This technique is commonly used to study the effects of Ang II on the morphology of the aorta as well as the functional and cytometric changes in the early stages. This model widely used in many studies (Daugherty and Cassis, 1999, Daugherty et al., 2000, Lu et al., 2015), has proven to be very reliable and

reproducible, and can recapitulate a vast number of characteristics of human aortic diseases.

Other methods of inducing vascular inflammation have been utilized in different studies, such as intra-aortic elastase perfusion or the application of calcium chloride peri-aortically. However, these methods require a laparotomy, which necessitates invasive surgery on the rodent (Pyo et al., 2000, Chiou et al., 2001). The method utilitzed in this study requires minimal surgical expertise to place the minipump in a subcutaneos pocket and close the wound using a criss-cross suture (Daugherty and Cassis, 1999, Daugherty et al., 2000).

The effect of Ang II on the groups of mice was clearly seen through MRI analysis. Regardless of their genetic backgrounds, the BL and d10 mice varied when the sectional areas of the aorta were quantified to identify the arterial lumen. However, in the male mice group, there was an intersection between sections 5 and 10 and around section 22, where the sectional lumen area of the d10 male mice was smaller than that of the BL group. This finding contradicts the established and aforementioned effects of Ang II and the results shown by various studies (Sawada et al., 2022, Police et al., 2010).

In a similar study conducted by Phillips et al., $ApoE^{-/-}$ rats were subcutaneously implanted with osmotic minipumps and analyzed via ultrasound. Similarly, no aortic dissections or AAA were observed after 56 days of Ang II infusion, and the overall size and morphology were relatively normal even after a prolonged Ang II infusion compared to our study of 10 days (Phillips et al., 2018).

In the female mice group, a noticeable and significant increase in the aortic lumen was observed. According to Mathieu et al., regarding the increased susceptibilty to dilated cardiomyopathy while comparing male and female mice, the study states that the female mice showed a higher susceptibilty to AT1R activation, resulting in more ventricular hypertrophy, dilation and mortality (Mathieu et al., 2018). However, other studies contradict our findings and the previous study. Xue et al. demonstrated a slightly diminished pressor response in female mice to Ang II compared to male mice (Xue et al., 2005, Xue et al., 2007), and further research in rats showed the same results (Tatchum-Talom et al., 2005, Ebrahimian et al., 2007).

The total aortic area was determined and compared for all groups. As anticipated, there was roughly a 1.2x increase in the overall area between the BL and d10 female mice, which correlates with the MRI flash scans. This difference was statistically significant when comparing the BL female group with all other groups. There was no difference between the male mice in the BL and d10 groups; hence, Ang II had no effect on the morphology of the aorta in the male group. The BL aortic total area of the male mice is significantly larger than that of the female mice due to the anatomical differences. The total area of the d10 male and female mice was nearly the same, making them quite comparable.

In order to assess the strain and velocity of the animals before and after Ang II treatment, the aortas were once more examined using ultrasound. Based on the findings, there was no discernible variation in strain between male and female mice (BL vs. d10), which further reinforces the findings that Ang II does not alter the morphology of the aorta, as seen in previous studies (Sawada et al., 2022). In a similar study conducted by Cao et al., 37% (amounting to 24 mice) did not develop a detectable AAA according to standard criteria, although Ang II was fully released into the system (Cao et al., 2010).

Between the female mice before and after the Ang II treatment, there was a small but not statistically significant drop in the mean velocity. In this regard, Gasparo et al. described an activation of AT2 receptors, particularly those located in the kidney, which enhanced the production of vasodilative NO and may account for this drop in blood flow velocity (de Gasparo and Siragy, 1999). The male group did not experience this, but in contrast, a modest increase in velocity was noted. There is a statistically significant difference between the velocity of male and female mice, with male mice exhibiting almost twice the velocity, which was also seen in the study published by our team (Massold et al., 2023).

The cytometric analysis showed noticeable differences between the BL and the d10 mice. Almost twice as many immune cells infiltrated the aorta in both female and male mice (significant difference), highlighting the effect of Ang II on the development of vascular inflammation. De Lima et al. demonstrated in an experimental study, where mice were injected intraperitoneally with 30ng/kg of Ang II, that there would be a vascular inflammatory response. After 30 minutes, an increase in CD45-positive cells was noticed, through the increase in the number of leukocytes, hence demonstrating the

involvement of innate immunity to this stimulus (de Lima et al., 2019). Similarly, Guzik et al. showed that animals given Ang II had higher levels of CD45 in their aorta (Guzik et al., 2007).

A slight increase in myeloid cells was observed in the female group, but this increase was significant in the male group. More siginificant, however, were the changes in lymphoid cells, which showed substantial increases in all groups and between female and male mice. The neutrophils exhibited a threefold increase in the d10 male mice compared to the BL male mice (500 vs. 1500), while no significant increase was observed within the female group. Significant differences were also seen in T and B-cell groups between the male group and between the female d10 and male d10 regarding the B-cells. Ang II has been previously linked to increased T-cell proliferation (Nataraj et al., 1999). For instance, Ang II increases CCR7 expression and differentiation, dendritic cell migration, and T-cell activation (Muller et al., 2002). It is also conceivable that oxidatively damaged lipoproteins or fatty acids produced from fat cells surrounding the arteries gain antigenic characteristics and are presented by dendritic cells to activate T-cell receptors (Kabelitz, 2007, Parks et al., 2006). Furthermore, Ang II might enhance immune responses to pathogens commonly encountered from the skin and gut, linking these frequent inflammatory processes to hypertension. TNF-α and IFN-γ production by T-cells is also stimulated by Ang II, suggesting the involvement of both innate and adaptive immunity (Guzik et al., 2007, Barhoumi et al., 2011, Shao et al., 2003).

Notably, neutrophils are considered significant effector cells in the innate arm of the immune system (Mayadas et al., 2014). Our findings are consistent with a study by Mellak et al., which showed that neutrophils were recruited into the vessel wall early and characterized by cytokine release, NET formation, and granule protein secretion in mice that did not develop AAA after Ang II exposure (Raffort et al., 2017, Soehnlein et al., 2009).

Gender has been shown to have a clinical impact on the development of AAA, in addition to other risk factors such as family history, advanced age, hypertension, atherosclerosis, smoking history, and chronic obstructive pulmonary disease (COPD) (Lederle et al., 2000, Alcorn et al., 1996). A study by Lederle et al. demonstrated that the most significant relationships with AAA are identical to those reported in men despite the substantially lower prevalence of AAA in women (Lederle et al., 2001).

Various previous studies have shown that females demonstrate a greater AT2R to AT1R balance than males (Armando et al., 2002, Mirabito et al., 2014, Baiardi et al., 2005, Silva-Antonialli et al., 2004), which means that the expression of multiple depressor pathways such as ACE2, AT2R, or Ang(1-7) of the RAAS is enhanced in females (Hilliard et al., 2013). According to Bosnyak et al., Ang II has a 15-fold greater affinity for the AT2R than the AT1R (Bosnyak et al., 2011). As a result, when female rodents are infused with Ang II, it binds more strongly to the AT2R than the AT1R. Furthermore, Ang III and Ang(1-7), which are generated from Ang II, both activate the AT2R to lead to a decrease in arterial pressure (Padia et al., 2008, Castro et al., 2005, Kemp et al., 2012). In other animal models of arterial pressure and hypertension measurements, males have been shown to have higher blood pressure compared to females (Brosnihan et al., 1997, Chen, 1996, Rowland and Fregly, 1992).

The last subgroup was analyzed to compare the effects of the Ang II infusion in both female and male groups, focusing on the early effects of AAA and vascular inflammation to determine if both gender and genetic background play a role. The MRI scans did not reveal any significant differences across all groups, indicating no significant gender-related difference in aortic size post-Ang II treatment. This finding underscores the reliability of this model in examining the early stages of vascular disease.

The ultrasound measurements revealed an interesting phenomenon. The strain of the $CD73^{-/-}$ female group was less than that of the $CD73^{+/+}$ group, while an increase was noticed in the male group. This observation is well-documented in numerous studies, where males consistently exhibit higher blood pressure compared to females in experimental models of hypertension, including those involving Ang II infusion (Sandberg and Ji, 2012, Sartori-Valinotti et al., 2008). Regarding velocity, both $CD73^{+/+}$ groups, of both sexes, showed higher velocities than their $CD73^{-/-}$ counterparts. Gasparo's study provides a compelling explanation for the reduction in blood flow velocity, suggesting it is due to the secretion of nitric oxide (NO), which subsequently induces vasodilation of the vasculature (de Gasparo and Siragy, 1999).

The cytometric analysis revealed no significant differences between the male and female groups. However, slight fluctuations were observed among the different genetic backgrounds, which displayed similar patterns in both genders. Notably, $CD73^{+/+}$ male

mice exhibited a higher T-cell count compared to $CD73^{+/+}$ female mice, consistent with findings from a 2015 study (Zimmerman et al., 2015). Despite these observations, the lack of statistical significance in the results suggests that neither sex nor genetic background plays a decisive role in the early stages of AAA, even with Ang II treatment.

Lastly, the expression of CD73 on the total immune cells found in the aortic wall of CD73+/+ mice notably decreased following Ang II treatment. Specifically, a downregulation of CD73 was observed in neutrophils and macrophages, whereas T and B cells showed minimal changes. This reduction in CD73 expression in neutrophils and macrophages under Ang II treatment suggests that these cells in wildtype animals exhibit a $CD73^{-/-}$ phenotype, which is associated with a proinflammatory milieu. This may account for why CD73-/- animals do not show increased inflammation compared to the CD73+/+ strain (Massold et al., 2023). A randomized, double-blind, placebo-controlled study reported that upregulation of CD73 was significantly associated with improved survival following emergency aortic reconstruction after AAA rupture. This finding suggests that CD73 could be a potential therapeutic target for achieving more favorable outcomes post-surgery (Hakovirta et al., 2022).

Our comprehensive characterization of the model following short-term treatment, combined with the utilization of multiple assessment techniques, has demonstrated its effectiveness in studying the early mechanisms involved in the development of aortic diseases. This knowledge contributes to a better understanding of the impact of Ang II treatment on vascular inflammation, immune cell infiltration, and hemodynamic changes. Concluding that hormones operate via the same mechanism in both males and females based solely on similar blood pressure effects is not valid. Additionally, the underlying pathology, dosage or combination of agents, age, and other factors likely influence whether the effects of gonadal steroids are beneficial or adverse.

The formation of aortic disease is influenced by various manipulable and non-manipulable risk factors, with gender being a significant non-manipulable factor. Men are more frequently affected by this disease than women (Li et al., 2013). However, our study found that gender did not influence disease development in the absence of CD73, nor did we observe any CD73-related gender-specific changes in vessel physiology or immune cell distribution. These findings suggest that inhibiting CD73 will not interfere

with these risk factors. This is particularly relevant for several clinical trials exploring CD73 inhibition for cancer treatment (Geoghegan et al., 2016, Perrot et al., 2019). Patients undergoing CD73 inhibition should not face an increased risk of developing aortic disease.

While our study has limitations, including the absence of observed sex-dependent effects, the reduction in CD73 expression points to its potential as a therapeutic target. This underscores the need for more detailed investigations to explore the specific mechanisms through which CD73 influences inflammatory pathways within the vascular system. By addressing these gaps, future research could pave the way for novel interventions aimed at modulating CD73 activity, ultimately improving outcomes for patients with vascular inflammation and preventing the formation of AAA.

10. List of Figures

11. List of Tables

12. References

ABBRACCHIO, M. P., BURNSTOCK, G., VERKHRATSKY, A., et al. 2009. Purinergic signalling in the nervous system: an overview. *Trends Neurosci,* 32**,** 19-29.

ADAN, A., ALIZADA, G., KIRAZ, Y., et al. 2017. Flow cytometry: basic principles and applications. *Crit Rev Biotechnol,* 37**,** 163-176.

AFANASYEVA, M., GEORGAKOPOULOS, D., BELARDI, D. F., et al. 2004. Quantitative analysis of myocardial inflammation by flow cytometry in murine autoimmune myocarditis: correlation with cardiac function. *Am J Pathol,* 164**,** 807-15.

AHRENS, E. T. & BULTE, J. W. 2013. Tracking immune cells in vivo using magnetic resonance imaging. *Nat Rev Immunol,* 13**,** 755-63.

ALCORN, H. G., WOLFSON, S. K., JR., SUTTON-TYRRELL, K., et al. 1996. Risk factors for abdominal aortic aneurysms in older adults enrolled in The Cardiovascular Health Study. *Arterioscler Thromb Vasc Biol,* 16**,** 963-70.

ALMOSHARI, Y. 2022. Osmotic Pump Drug Delivery Systems-A Comprehensive Review. *Pharmaceuticals (Basel),* 15.

ALTOBELLI, E., RAPACCHIETTA, L., PROFETA, V. F., et al. 2018. Risk Factors for Abdominal Aortic Aneurysm in Population-Based Studies: A Systematic Review and Meta-Analysis. *Int J Environ Res Public Health,* 15.

ANDERSON, I. 1995. Doppler ultrasound recording of ankle brachial pressure index in the community. *J Wound Care,* 4**,** 325-7.

ANTONIOLI, L., PACHER, P., VIZI, E. S., et al. 2013. CD39 and CD73 in immunity and inflammation. *Trends Mol Med,* 19**,** 355-67.

ARMANDO, I., JEZOVA, M., JUORIO, A. V., et al. 2002. Estrogen upregulates renal angiotensin II AT(2) receptors. *Am J Physiol Renal Physiol,* 283**,** F934-43.

BÄCK, M., YURDAGUL, A., JR., TABAS, I., et al. 2019. Inflammation and its resolution in atherosclerosis: mediators and therapeutic opportunities. *Nat Rev Cardiol,* 16**,** 389-406.

BAIARDI, G., MACOVA, M., ARMANDO, I., et al. 2005. Estrogen upregulates renal angiotensin II AT1 and AT2 receptors in the rat. *Regul Pept,* 124**,** 7-17.

BALLESTEROS-YÁÑEZ, I., CASTILLO, C. A., MERIGHI, S., et al. 2018. The Role of Adenosine Receptors in Psychostimulant Addiction. *Frontiers in Pharmacology,* 8.

BARAN, J., PITUCH-NOWOROLSKA, A., KRZESZOWIAK, A., et al. 1998. Detection of cancer cells in the blood by FACS sorting of CD45- cells. *Int J Mol Med,* 1**,** 573-8.

BARHOUMI, T., KASAL, D. A., LI, M. W., et al. 2011. T regulatory lymphocytes prevent angiotensin II-induced hypertension and vascular injury. *Hypertension,* 57**,** 469-76.

BERK, B. C., HAENDELER, J. & SOTTILE, J. 2000. Angiotensin II, atherosclerosis, and aortic aneurysms. *J Clin Invest,* 105**,** 1525-6.

BERSI, M. R., ACOSTA SANTAMARÍA, V. A., MARBACK, K., et al. 2020. Multimodality Imaging-Based Characterization of Regional Material Properties in a Murine Model of Aortic Dissection. *Sci Rep,* 10**,** 9244.

BLACHE, U., WEISS, R., BOLDT, A., et al. 2021. Advanced Flow Cytometry Assays for Immune Monitoring of CAR-T Cell Applications. *Front Immunol,* 12**,** 658314.

BONANNO, E., MAURIELLO, A., PARTENZI, A., et al. 2000. Flow cytometry analysis of atherosclerotic plaque cells from human carotids: a validation study. *Cytometry,* 39**,** 158-65.

BORG, N., ALTER, C., GÖRLDT, N., et al. 2017. CD73 on T Cells Orchestrates Cardiac Wound Healing After Myocardial Infarction by Purinergic Metabolic Reprogramming. *Circulation,* 136**,** 297-313.

BORING, L., GOSLING, J., CLEARY, M., et al. 1998. Decreased lesion formation in CCR2-/- mice reveals a role for chemokines in the initiation of atherosclerosis. *Nature,* 394**,** 894-7.

BOSNYAK, S., JONES, E. S., CHRISTOPOULOS, A., et al. 2011. Relative affinity of angiotensin peptides and novel ligands at AT1 and AT2 receptors. *Clin Sci (Lond),* 121**,** 297-303.

BRANGSCH, J., REIMANN, C., KAUFMANN, J. O., et al. 2019. Concurrent Molecular Magnetic Resonance Imaging of Inflammatory Activity and Extracellular Matrix Degradation for the Prediction of Aneurysm Rupture. *Circ Cardiovasc Imaging,* 12**,** e008707.

BROSNIHAN, K. B., LI, P., GANTEN, D., et al. 1997. Estrogen protects transgenic hypertensive rats by shifting the vasoconstrictor-vasodilator balance of RAS. *Am J Physiol,* 273**,** R1908-15.

BROWN, L. C., POWELL, J. T., THOMPSON, S. G., et al. 2012. The UK EndoVascular Aneurysm Repair (EVAR) trials: randomised trials of EVAR versus standard therapy. *Health Technol Assess,* 16**,** 1-218.

BUCHHEISER, A., EBNER, A., BURGHOFF, S., et al. 2011. Inactivation of CD73 promotes atherogenesis in apolipoprotein E-deficient mice. *Cardiovasc Res,* 92**,** 338-47.

BURNSTOCK, G. 2012. Purinergic signalling: Its unpopular beginning, its acceptance and its exciting future. *Bioessays,* 34**,** 218-25.

BURRELL, L. M., CHAN, R., PHILLIPS, P. A., et al. 1996. Validation of an echocardiographic assessment of cardiac function following moderate size myocardial infarction in the rat. *Clin Exp Pharmacol Physiol,* 23**,** 570-2.

BURTEA, C., LAURENT, S., VANDER ELST, L., et al. 2008. Contrast agents: magnetic resonance. *Handb Exp Pharmacol***,** 135-65.

BUTCHER, M. J., HERRE, M., LEY, K., et al. 2011. Flow cytometry analysis of immune cells within murine aortas. *J Vis Exp*.

CAO, R. Y., AMAND, T., FORD, M. D., et al. 2010. The Murine Angiotensin II-Induced Abdominal Aortic Aneurysm Model: Rupture Risk and Inflammatory Progression Patterns. *Front Pharmacol,* 1**,** 9.

CASTRO, C. H., SANTOS, R. A., FERREIRA, A. J., et al. 2005. Evidence for a functional interaction of the angiotensin-(1-7) receptor Mas with AT1 and AT2 receptors in the mouse heart. *Hypertension,* 46**,** 937-42.

CHANDA, M. K., SHUDDE, C. E., PIPER, T. L., et al. 2022. Combined analysis of T cell activation and T cell-mediated cytotoxicity by imaging cytometry. *J Immunol Methods,* 506**,** 113290.

CHARO, I. F. & TAUB, R. 2011. Anti-inflammatory therapeutics for the treatment of atherosclerosis. *Nat Rev Drug Discov,* 10**,** 365-76.

CHEN, J. F., ELTZSCHIG, H. K. & FREDHOLM, B. B. 2013. Adenosine receptors as drug targets--what are the challenges? *Nat Rev Drug Discov,* 12**,** 265-86.

CHEN, L., DENG, H., CUI, H., et al. 2018. Inflammatory responses and inflammation-associated diseases in organs. *Oncotarget,* 9**,** 7204-7218.

CHEN, Y. F. 1996. Sexual dimorphism of hypertension. *Curr Opin Nephrol Hypertens,* 5**,** 181-5.

CHIOU, A. C., CHIU, B. & PEARCE, W. H. 2001. Murine aortic aneurysm produced by periarterial application of calcium chloride. *J Surg Res,* 99**,** 371-6.

CITTADINI, A., STRÖMER, H., KATZ, S. E., et al. 1996. Differential cardiac effects of growth hormone and insulin-like growth factor-1 in the rat. A combined in vivo and in vitro evaluation. *Circulation,* 93**,** 800-9.

CORNUZ, J., SIDOTI PINTO, C., TEVAEARAI, H., et al. 2004. Risk factors for asymptomatic abdominal aortic aneurysm: systematic review and meta-analysis of population-based screening studies. *Eur J Public Health,* 14**,** 343-9.

COSTANTINO, T. G., BRUNO, E. C., HANDLY, N., et al. 2005. Accuracy of emergency medicine ultrasound in the evaluation of abdominal aortic aneurysm. *J Emerg Med,* 29**,** 455-60.

CRONSTEIN, B. N., DAGUMA, L., NICHOLS, D., et al. 1990. The adenosine/neutrophil paradox resolved: human neutrophils possess both A1 and A2 receptors that promote chemotaxis and inhibit O2 generation, respectively. *J Clin Invest,* 85**,** 1150-7.

DALE, M. A., RUHLMAN, M. K. & BAXTER, B. T. 2015. Inflammatory cell phenotypes in AAAs: their role and potential as targets for therapy. *Arterioscler Thromb Vasc Biol,* 35**,** 1746-55.

DAUGHERTY, A. & CASSIS, L. 1999. Chronic angiotensin II infusion promotes atherogenesis in low density lipoprotein receptor -/- mice. *Ann N Y Acad Sci,* 892**,** 108-18.

DAUGHERTY, A., MANNING, M. W. & CASSIS, L. A. 2000. Angiotensin II promotes atherosclerotic lesions and aneurysms in apolipoprotein E-deficient mice. *J Clin Invest,* 105**,** 1605-12.

DAUGHERTY, A., MANNING, M. W. & CASSIS, L. A. 2001. Antagonism of AT2 receptors augments angiotensin II-induced abdominal aortic aneurysms and atherosclerosis. *Br J Pharmacol,* 134**,** 865-70.

DAVILA, D. 1992. [Therapeutic systems and drug delivery. 4. The osmotic minipump]. *Lijec Vjesn,* 114**,** 62-7.

DE GASPARO, M. & SIRAGY, H. M. 1999. The AT2 receptor: fact, fancy and fantasy. *Regul Pept,* 81**,** 11-24.

DE LIMA, R. S., SILVA, J. C. S., LIMA, C. T., et al. 2019. Proinflammatory Role of Angiotensin II in the Aorta of Normotensive Mice. *Biomed Res Int,* 2019**,** 9326896.

EBNER, B., BEHM, P., JACOBY, C., et al. 2010. Early assessment of pulmonary inflammation by 19F MRI in vivo. *Circ Cardiovasc Imaging,* 3**,** 202-10.

EBRAHIMIAN, T., HE, Y., SCHIFFRIN, E. L., et al. 2007. Differential regulation of thioredoxin and NAD(P)H oxidase by angiotensin II in male and female mice. *J Hypertens,* 25**,** 1263-71.

ECKLE, T., FAIGLE, M., GRENZ, A., et al. 2008. A2B adenosine receptor dampens hypoxia-induced vascular leak. *Blood,* 111**,** 2024-35.

ECKLE, T., KRAHN, T., GRENZ, A., et al. 2007. Cardioprotection by ecto-5'-nucleotidase (CD73) and A2B adenosine receptors. *Circulation,* 115**,** 1581-90.

EICHIN, D., PESSIA, A., TAKEDA, A., et al. 2021. CD73 contributes to anti-inflammatory properties of afferent lymphatic endothelial cells in humans and mice. *Eur J Immunol,* 51**,** 231-246.

ERDMANN, A. A., GAO, Z. G., JUNG, U., et al. 2005. Activation of Th1 and Tc1 cell adenosine A2A receptors directly inhibits IL-2 secretion in vitro and IL-2-driven expansion in vivo. *Blood,* 105**,** 4707-14.

ERNST, P. B., GARRISON, J. C. & THOMPSON, L. F. 2010. Much ado about adenosine: adenosine synthesis and function in regulatory T cell biology. *J Immunol,* 185**,** 1993-8.

FENG, L.-L., CAI, Y.-Q., ZHU, M.-C., et al. 2020. The yin and yang functions of extracellular ATP and adenosine in tumor immunity. *Cancer Cell International,* 20**,** 110.

FILARDO, G., POWELL, J. T., MARTINEZ, M. A., et al. 2015. Surgery for small asymptomatic abdominal aortic aneurysms. *Cochrane Database Syst Rev,* 2015**,** Cd001835.

FLEMING, C., WHITLOCK, E. P., BEIL, T. L., et al. 2005. Screening for abdominal aortic aneurysm: a best-evidence systematic review for the U.S. Preventive Services Task Force. *Ann Intern Med,* 142**,** 203-11.

FLÖGEL, U., DING, Z., HARDUNG, H., et al. 2008. In vivo monitoring of inflammation after cardiac and cerebral ischemia by fluorine magnetic resonance imaging. *Circulation,* 118**,** 140-8.

FORMAN, D. E., CITTADINI, A., AZHAR, G., et al. 1997. Cardiac morphology and function in senescent rats: gender-related differences. *J Am Coll Cardiol,* 30**,** 1872-7.

FREDHOLM, B. B., AP, I. J., JACOBSON, K. A., et al. 2001. International Union of Pharmacology. XXV. Nomenclature and classification of adenosine receptors. *Pharmacol Rev,* 53**,** 527-52.

FYHRQUIST, F., METSÄRINNE, K. & TIKKANEN, I. 1995. Role of angiotensin II in blood pressure regulation and in the pathophysiology of cardiovascular disorders. *J Hum Hypertens,* 9 Suppl 5**,** S19-24.

GALKINA, E., KADL, A., SANDERS, J., et al. 2006. Lymphocyte recruitment into the aortic wall before and during development of atherosclerosis is partially L-selectin dependent. *J Exp Med,* 203**,** 1273-82.

GEOGHEGAN, J. C., DIEDRICH, G., LU, X., et al. 2016. Inhibition of CD73 AMP hydrolysis by a therapeutic antibody with a dual, non-competitive mechanism of action. *MAbs,* 8**,** 454-67.

GOLLEDGE, J. & NORMAN, P. E. 2010. Atherosclerosis and abdominal aortic aneurysm: cause, response, or common risk factors? *Arterioscler Thromb Vasc Biol,* 30**,** 1075-7.

GRAEVE, A. H., CARPENTER, C. M., WICKS, J. D., et al. 1982. Discordance in the sizing of abdominal aortic aneurysm and its significance. *Am J Surg,* 144**,** 627-34.

GRIENDLING, K. K., MINIERI, C. A., OLLERENSHAW, J. D., et al. 1994. Angiotensin II stimulates NADH and NADPH oxidase activity in cultured vascular smooth muscle cells. *Circ Res,* 74**,** 1141-8.

GUZIK, T. J., HOCH, N. E., BROWN, K. A., et al. 2007. Role of the T cell in the genesis of angiotensin II induced hypertension and vascular dysfunction. *J Exp Med,* 204**,** 2449-60.

HAKOVIRTA, H., JALKANEN, J., SAIMANEN, E., et al. 2022. Induction of CD73 prevents death after emergency open aortic surgery for a ruptured abdominal aortic aneurysm: a randomized, double-blind, placebo-controlled study. *Sci Rep,* 12**,** 1839.

HAMMOND, T. G. 1992. Analysis and isolation of renal tubular cells by flow cytometry. *Kidney Int,* 42**,** 997-1005.

HARVEY, J. B., PHAN, L. H., VILLARREAL, O. E., et al. 2020. CD73's Potential as an Immunotherapy Target in Gastrointestinal Cancers. *Frontiers in Immunology,* 11.

HASKÓ, G. & CRONSTEIN, B. 2013. Regulation of inflammation by adenosine. *Front Immunol,* 4**,** 85.

HASKÓ, G., CSÓKA, B., KOSCSÓ, B., et al. 2011. Ecto-5'-nucleotidase (CD73) decreases mortality and organ injury in sepsis. *J Immunol,* 187**,** 4256-67.

HATTANGADY, N. G., OLALA, L. O., BOLLAG, W. B., et al. 2012. Acute and chronic regulation of aldosterone production. *Mol Cell Endocrinol,* 350**,** 151-62.

HESS, J. R. & GREENBERG, N. A. 2012. The role of nucleotides in the immune and gastrointestinal systems: potential clinical applications. *Nutr Clin Pract,* 27**,** 281-94.

HILLIARD, L. M., SAMPSON, A. K., BROWN, R. D., et al. 2013. The "his and hers" of the renin-angiotensin system. *Curr Hypertens Rep,* 15**,** 71-9.

HOFFMAN, R. A. & HANSEN, W. P. 1981. Immunofluorescent analysis of blood cells by flow cytometry. *Int J Immunopharmacol,* 3**,** 249-54.

HU, J., ZHENG, Z. F., ZHOU, X. T., et al. 2022. Normal diameters of abdominal aorta and common iliac artery in middle-aged and elderly Chinese Han people based on CTA. *Medicine (Baltimore),* 101**,** e30026.

JOHNSTON, K. W., RUTHERFORD, R. B., TILSON, M. D., et al. 1991. Suggested standards for reporting on arterial aneurysms. Subcommittee on Reporting Standards for Arterial Aneurysms, Ad Hoc Committee on Reporting Standards, Society for Vascular Surgery and North American Chapter, International Society for Cardiovascular Surgery. *J Vasc Surg,* 13**,** 452-8.

JUNGER, W. G. 2011. Immune cell regulation by autocrine purinergic signalling. *Nat Rev Immunol,* 11**,** 201-12.

KABELITZ, D. 2007. Expression and function of Toll-like receptors in T lymphocytes. *Curr Opin Immunol,* 19**,** 39-45.

KEISLER, B. & CARTER, C. 2015. Abdominal aortic aneurysm. *Am Fam Physician,* 91**,** 538-43.

KEMP, B. A., BELL, J. F., ROTTKAMP, D. M., et al. 2012. Intrarenal angiotensin III is the predominant agonist for proximal tubule angiotensin type 2 receptors. *Hypertension,* 60**,** 387-95.

KENT, K. C., ZWOLAK, R. M., EGOROVA, N. N., et al. 2010. Analysis of risk factors for abdominal aortic aneurysm in a cohort of more than 3 million individuals. *J Vasc Surg,* 52**,** 539-48.

KIM, H., CHO, S., SAKALIHASAN, N., et al. 2023. Prevalence and Risk Factors of Abdominal Aortic Aneurysms Detected with Ultrasound in Korea and Belgium. *J Clin Med,* 12.

KLINK, A., HEYNENS, J., HERRANZ, B., et al. 2011. In vivo characterization of a new abdominal aortic aneurysm mouse model with conventional and molecular magnetic resonance imaging. *J Am Coll Cardiol,* 58**,** 2522-30.

KOLTSOVA, E. K., GARCIA, Z., CHODACZEK, G., et al. 2012. Dynamic T cell-APC interactions sustain chronic inflammation in atherosclerosis. *J Clin Invest,* 122**,** 3114-26.

KRAUSE, M. W., FONSECA, V. A. & SHAH, S. V. 2011. Combination inhibition of the renin-angiotensin system: is more better? *Kidney Int,* 80**,** 245-55.

KRECKLER, L. M., WAN, T. C., GE, Z. D., et al. 2006. Adenosine inhibits tumor necrosis factor-alpha release from mouse peritoneal macrophages via A2A and A2B but not the A3 adenosine receptor. *J Pharmacol Exp Ther,* 317**,** 172-80.

KRISHNA, S. M., MORTON, S. K., LI, J., et al. 2020. Risk Factors and Mouse Models of Abdominal Aortic Aneurysm Rupture. *Int J Mol Sci,* 21.

KÜHNL, A., ERK, A., TRENNER, M., et al. 2017. Incidence, Treatment and Mortality in Patients with Abdominal Aortic Aneurysms. *Dtsch Arztebl Int,* 114**,** 391-398.

KUIVANIEMI, H., RYER, E. J., ELMORE, J. R., et al. 2015. Understanding the pathogenesis of abdominal aortic aneurysms. *Expert Rev Cardiovasc Ther,* 13**,** 975-87.

KUROKI, M. T., FINK, G. D. & OSBORN, J. W. 2014. Comparison of arterial pressure and plasma ANG II responses to three methods of subcutaneous ANG II administration. *Am J Physiol Heart Circ Physiol,* 307**,** H670-9.

LEDERLE, F. A., JOHNSON, G. R. & WILSON, S. E. 2001. Abdominal aortic aneurysm in women. *J Vasc Surg,* 34**,** 122-6.

LEDERLE, F. A., JOHNSON, G. R., WILSON, S. E., et al. 2000. The aneurysm detection and management study screening program: validation cohort and final results. Aneurysm Detection and Management Veterans Affairs Cooperative Study Investigators. *Arch Intern Med,* 160**,** 1425-30.

LEDERLE, F. A., JOHNSON, G. R., WILSON, S. E., et al. 1997. Relationship of age, gender, race, and body size to infrarenal aortic diameter. The Aneurysm Detection and Management (ADAM) Veterans Affairs Cooperative Study Investigators. *J Vasc Surg,* 26**,** 595-601.

LEDERLE, F. A., WALKER, J. M. & REINKE, D. B. 1988. Selective screening for abdominal aortic aneurysms with physical examination and ultrasound. *Arch Intern Med,* 148**,** 1753-6.

LEE, S. H., KIM, B. H., NA, H. B., et al. 2014. Paramagnetic inorganic nanoparticles as T1 MRI contrast agents. *Wiley Interdiscip Rev Nanomed Nanobiotechnol,* 6**,** 196-209.

LEFEVRE, M. L. 2014. Screening for abdominal aortic aneurysm: U.S. Preventive Services Task Force recommendation statement. *Ann Intern Med,* 161**,** 281-90.

LEY, K., LAUDANNA, C., CYBULSKY, M. I., et al. 2007. Getting to the site of inflammation: the leukocyte adhesion cascade updated. *Nat Rev Immunol,* 7**,** 678-89.

LI, X., ZHAO, G., ZHANG, J., et al. 2013. Prevalence and trends of the abdominal aortic aneurysms epidemic in general population--a meta-analysis. *PLoS One,* 8**,** e81260.

LINDEN, J. 2006. New insights into the regulation of inflammation by adenosine. *J Clin Invest,* 116**,** 1835-7.

LINDHOLT, J. S., VAMMEN, S., JUUL, S., et al. 1999. The validity of ultrasonographic scanning as screening method for abdominal aortic aneurysm. *Eur J Vasc Endovasc Surg,* 17**,** 472-5.

LITWIN, S. E., KATZ, S. E., MORGAN, J. P., et al. 1994. Serial echocardiographic assessment of left ventricular geometry and function after large myocardial infarction in the rat. *Circulation,* 89**,** 345-54.

LIU-WU, Y., SVENNINGSSON, A., STEMME, S., et al. 1997. Identification and analysis of macrophage-derived foam cells from human atherosclerotic lesions by using a "mock" FL3 channel in flow cytometry. *Cytometry,* 29**,** 155-64.

LU, H., HOWATT, D. A., BALAKRISHNAN, A., et al. 2015. Subcutaneous Angiotensin II Infusion using Osmotic Pumps Induces Aortic Aneurysms in Mice. *J Vis Exp*.

MASSOLD, T., IBRAHIM, F., NIEMANN, V., et al. 2023. CD73 deficiency does not aggravate angiotensin II-induced aortic inflammation in mice. *Sci Rep,* 13**,** 17125.

MATHIEU, S., EL KHOURY, N., RIVARD, K., et al. 2018. Angiotensin II Overstimulation Leads to an Increased Susceptibility to Dilated Cardiomyopathy and Higher Mortality in Female Mice. *Sci Rep,* 8**,** 952.

MATTSSON, L., BONDJERS, G. & WIKLUND, O. 1991. Isolation of cell populations from arterial tissue, using monoclonal antibodies and magnetic microspheres. *Atherosclerosis,* 89**,** 25-34.

MAYADAS, T. N., CULLERE, X. & LOWELL, C. A. 2014. The multifaceted functions of neutrophils. *Annu Rev Pathol,* 9**,** 181-218.

MCKINNON, K. M. 2018. Flow Cytometry: An Overview. *Curr Protoc Immunol,* 120**,** 5.1.1-5.1.11.

MEDZHITOV, R. 2008. Origin and physiological roles of inflammation. *Nature,* 454**,** 428-35.

MELLAK, S., AIT-OUFELLA, H., ESPOSITO, B., et al. 2015. Angiotensin II mobilizes spleen monocytes to promote the development of abdominal aortic aneurysm in Apoe-/- mice. *Arterioscler Thromb Vasc Biol,* 35**,** 378-88.

MEYENBURG, M., LANG, R., SALING, E., et al. 1990. Does pulsed-Doppler ultrasound have mutagenic effects? Application of the Ames mutagenicity assay to test pulsed-Doppler equipment. *Echocardiography,* 7**,** 657-60.

MIRABITO, K. M., HILLIARD, L. M., KETT, M. M., et al. 2014. Sex- and age-related differences in the chronic pressure-natriuresis relationship: role of the angiotensin type 2 receptor. *Am J Physiol Renal Physiol,* 307**,** F901-7.

MOLL, F. L., POWELL, J. T., FRAEDRICH, G., et al. 2011. Management of abdominal aortic aneurysms clinical practice guidelines of the European society for vascular surgery. *Eur J Vasc Endovasc Surg,* 41 Suppl 1**,** S1-S58.

MULLER, D. N., SHAGDARSUREN, E., PARK, J. K., et al. 2002. Immunosuppressive treatment protects against angiotensin II-induced renal damage. *Am J Pathol,* 161**,** 1679-93.

NAGANUMA, M., WIZNEROWICZ, E. B., LAPPAS, C. M., et al. 2006. Cutting edge: Critical role for A2A adenosine receptors in the T cell-mediated regulation of colitis. *J Immunol,* 177**,** 2765-9.

NATARAJ, C., OLIVERIO, M. I., MANNON, R. B., et al. 1999. Angiotensin II regulates cellular immune responses through a calcineurin-dependent pathway. *J Clin Invest,* 104**,** 1693-701.

NISHAT, S., KHAN, L. A., ANSARI, Z. M., et al. 2016. Adenosine A3 Receptor: A promising therapeutic target in cardiovascular disease. *Curr Cardiol Rev,* 12**,** 18-26.

PADIA, S. H., KEMP, B. A., HOWELL, N. L., et al. 2008. Conversion of renal angiotensin II to angiotensin III is critical for AT2 receptor-mediated natriuresis in rats. *Hypertension,* 51**,** 460-5.

PARKER, R. B. & MCCOLLAM, P. L. 1990. Adenosine in the episodic treatment of paroxysmal supraventricular tachycardia. *Clin Pharm,* 9**,** 261-71.

PARKS, B. W., LUSIS, A. J. & KABAROWSKI, J. H. 2006. Loss of the lysophosphatidylcholine effector, G2A, ameliorates aortic atherosclerosis in low-density lipoprotein receptor knockout mice. *Arterioscler Thromb Vasc Biol,* 26**,** 2703-9.

PATEL, P., SANGHAVI, D. K., MORRIS, D. L., et al. 2024. Angiotensin II. *StatPearls.* Treasure Island (FL): StatPearls Publishing

Copyright © 2024, StatPearls Publishing LLC.

PERROT, I., MICHAUD, H. A., GIRAUDON-PAOLI, M., et al. 2019. Blocking Antibodies Targeting the CD39/CD73 Immunosuppressive Pathway Unleash Immune Responses in Combination Cancer Therapies. *Cell Rep,* 27**,** 2411-2425.e9.

PHAM, M. H. C., BALLEGAARD, C., DE KNEGT, M. C., et al. 2019. Normal values of aortic dimensions assessed by multidetector computed tomography in the Copenhagen General Population Study. *Eur Heart J Cardiovasc Imaging,* 20**,** 939-948.

PHILLIPS, E. H., CHANG, M. S., GORMAN, S., et al. 2018. Angiotensin II Infusion Does Not Cause Abdominal Aortic Aneurysms in Apolipoprotein E-Deficient Rats. *J Vasc Res,* 55**,** 1-12.

POLICE, S. B., PUTNAM, K., THATCHER, S., et al. 2010. Weight loss in obese C57BL/6 mice limits adventitial expansion of established angiotensin II-induced abdominal aortic aneurysms. *Am J Physiol Heart Circ Physiol,* 298**,** H1932-8.

PYO, R., LEE, J. K., SHIPLEY, J. M., et al. 2000. Targeted gene disruption of matrix metalloproteinase-9 (gelatinase B) suppresses development of experimental abdominal aortic aneurysms. *J Clin Invest,* 105**,** 1641-9.

QUAST, C., ALTER, C., DING, Z., et al. 2017. Adenosine Formed by CD73 on T Cells Inhibits Cardiac Inflammation and Fibrosis and Preserves Contractile Function in Transverse Aortic Constriction-Induced Heart Failure. *Circ Heart Fail,* 10.

QUILL, D. S., COLGAN, M. P. & SUMNER, D. S. 1989. Ultrasonic screening for the detection of abdominal aortic aneurysms. *Surg Clin North Am,* 69**,** 713-20.

RAFFORT, J., LAREYRE, F., CLÉMENT, M., et al. 2017. Monocytes and macrophages in abdominal aortic aneurysm. *Nat Rev Cardiol,* 14**,** 457-471.

RAJAGOPALAN, S., KURZ, S., MÜNZEL, T., et al. 1996. Angiotensin II-mediated hypertension in the rat increases vascular superoxide production via membrane NADH/NADPH oxidase activation. Contribution to alterations of vasomotor tone. *J Clin Invest,* 97**,** 1916-23.

ROGERS, I. S., MASSARO, J. M., TRUONG, Q. A., et al. 2013. Distribution, determinants, and normal reference values of thoracic and abdominal aortic diameters by computed tomography (from the Framingham Heart Study). *Am J Cardiol,* 111**,** 1510-6.

ROWLAND, N. E. & FREGLY, M. J. 1992. Role of gonadal hormones in hypertension in the Dahl salt-sensitive rat. *Clin Exp Hypertens A,* 14**,** 367-75.

RUBANO, E., MEHTA, N., CAPUTO, W., et al. 2013. Systematic review: emergency department bedside ultrasonography for diagnosing suspected abdominal aortic aneurysm. *Acad Emerg Med,* 20**,** 128-38.

RUIZ-ORTEGA, M., RUPEREZ, M., LORENZO, O., et al. 2002. Angiotensin II regulates the synthesis of proinflammatory cytokines and chemokines in the kidney. *Kidney Int Suppl***,** S12-22.

SAKALIHASAN, N., LIMET, R. & DEFAWE, O. D. 2005. Abdominal aortic aneurysm. *Lancet,* 365**,** 1577-89.

SAKALIHASAN, N., MICHEL, J. B., KATSARGYRIS, A., et al. 2018. Abdominal aortic aneurysms. *Nat Rev Dis Primers,* 4**,** 34.

SANDBERG, K. & JI, H. 2012. Sex differences in primary hypertension. *Biol Sex Differ,* 3**,** 7.

SAREEN, R., JAIN, N. & KUMAR, D. 2012. An insight to osmotic drug delivery. *Curr Drug Deliv,* 9**,** 285-96.

SARTORI-VALINOTTI, J. C., ILIESCU, R., YANES, L. L., et al. 2008. Sex differences in the pressor response to angiotensin II when the endogenous renin-angiotensin system is blocked. *Hypertension,* 51**,** 1170-6.

SAWADA, H., LU, H. S., CASSIS, L. A., et al. 2022. Twenty Years of Studying AngII (Angiotensin II)-Induced Abdominal Aortic Pathologies in Mice: Continuing Questions and Challenges to Provide Insight Into the Human Disease. *Arterioscler Thromb Vasc Biol,* 42**,** 277-288.

SCHÄBERLE, W., LEYERER, L., SCHIERLING, W., et al. 2015. Ultrasound diagnostics of the abdominal aorta: English version. *Gefasschirurgie,* 20**,** 22-27.

SHAO, J., NANGAKU, M., MIYATA, T., et al. 2003. Imbalance of T-cell subsets in angiotensin II-infused hypertensive rats with kidney injury. *Hypertension,* 42**,** 31-8.

SILVA-ANTONIALLI, M. M., TOSTES, R. C., FERNANDES, L., et al. 2004. A lower ratio of AT1/AT2 receptors of angiotensin II is found in female than in male spontaneously hypertensive rats. *Cardiovasc Res,* 62**,** 587-93.

SMITH, E., PRASAD, K. M., BUTCHER, M., et al. 2010. Blockade of interleukin-17A results in reduced atherosclerosis in apolipoprotein E-deficient mice. *Circulation,* 121**,** 1746-55.

SOEHNLEIN, O., LINDBOM, L. & WEBER, C. 2009. Mechanisms underlying neutrophil-mediated monocyte recruitment. *Blood,* 114**,** 4613-23.

SPARKS, M. A., CROWLEY, S. D., GURLEY, S. B., et al. 2014. Classical Renin-Angiotensin system in kidney physiology. *Compr Physiol,* 4**,** 1201-28.

SPROUSE, L. R., 2ND, MEIER, G. H., 3RD, PARENT, F. N., et al. 2004. Is ultrasound more accurate than axial computed tomography for determination of maximal abdominal aortic aneurysm diameter? *Eur J Vasc Endovasc Surg,* 28**,** 28-35.

STEUDEL, W., SCHERRER-CROSBIE, M., BLOCH, K. D., et al. 1998. Sustained pulmonary hypertension and right ventricular hypertrophy after chronic hypoxia in mice with congenital deficiency of nitric oxide synthase 3. *J Clin Invest,* 101**,** 2468-77.

STRUYKER-BOUDIER, H. A. & SMITS, J. F. 1978. The osmotic minipump: a new tool in the study of steady-state kinetics of drug distribution and metabolism. *J Pharm Pharmacol,* 30**,** 576-8.

SUH, Y. A., ARNOLD, R. S., LASSEGUE, B., et al. 1999. Cell transformation by the superoxide-generating oxidase Mox1. *Nature,* 401**,** 79-82.

SUTTON, N. R., BOUÏS, D., MANN, K. M., et al. 2020. CD73 Promotes Age-Dependent Accretion of Atherosclerosis. *Arterioscler Thromb Vasc Biol,* 40**,** 61-71.

TADA, Y., WADA, K., SHIMADA, K., et al. 2014. Roles of hypertension in the rupture of intracranial aneurysms. *Stroke,* 45**,** 579-86.

TANAKA, N., DALTON, N., MAO, L., et al. 1996. Transthoracic echocardiography in models of cardiac disease in the mouse. *Circulation,* 94**,** 1109-17.

TATCHUM-TALOM, R., EYSTER, K. M. & MARTIN, D. S. 2005. Sexual dimorphism in angiotensin II-induced hypertension and vascular alterations. *Can J Physiol Pharmacol,* 83**,** 413-22.

TAYAL, V. S., GRAF, C. D. & GIBBS, M. A. 2003. Prospective study of accuracy and outcome of emergency ultrasound for abdominal aortic aneurysm over two years. *Acad Emerg Med,* 10**,** 867-71.

THEEUWES, F. & YUM, S. I. 1976. Principles of the design and operation of generic osmotic pumps for the delivery of semisolid or liquid drug formulations. *Ann Biomed Eng,* 4**,** 343-53.

THOMPSON, L. F., ELTZSCHIG, H. K., IBLA, J. C., et al. 2004. Crucial role for ecto-5'-nucleotidase (CD73) in vascular leakage during hypoxia. *J Exp Med,* 200**,** 1395-405.

TIROTTA, I., DICHIARANTE, V., PIGLIACELLI, C., et al. 2015. (19)F magnetic resonance imaging (MRI): from design of materials to clinical applications. *Chem Rev,* 115**,** 1106-29.

TRACEY, W. R., MAGEE, W., MASAMUNE, H., et al. 1998. Selective activation of adenosine A3 receptors with N6-(3-chlorobenzyl)-5'-N-methylcarboxamidoadenosine (CB-MECA) provides cardioprotection via KATP channel activation. *Cardiovasc Res,* 40**,** 138-45.

TUMMALA, P. E., CHEN, X. L., SUNDELL, C. L., et al. 1999. Angiotensin II induces vascular cell adhesion molecule-1 expression in rat vasculature: A potential link between the renin-angiotensin system and atherosclerosis. *Circulation,* 100**,** 1223-9.

TURNER, G. H., OLZINSKI, A. R., BERNARD, R. E., et al. 2008. In vivo serial assessment of aortic aneurysm formation in apolipoprotein E-deficient mice via MRI. *Circ Cardiovasc Imaging,* 1**,** 220-6.

VAN DER HOEVEN, D., WAN, T. C., GIZEWSKI, E. T., et al. 2011. A role for the low-affinity A2B adenosine receptor in regulating superoxide generation by murine neutrophils. *J Pharmacol Exp Ther,* 338**,** 1004-12.

VESTWEBER, D. 2012. Relevance of endothelial junctions in leukocyte extravasation and vascular permeability. *Ann N Y Acad Sci,* 1257**,** 184-92.

VON ALLMEN, R. S. & POWELL, J. T. 2012. The management of ruptured abdominal aortic aneurysms: screening for abdominal aortic aneurysm and incidence of rupture. *J Cardiovasc Surg (Torino),* 53**,** 69-76.

WAZZAN, M., ABDULJABBAR, A., AJLAN, A., et al. 2022. Reference for Normal Diameters of the Abdominal Aorta and Common Iliac Arteries in the Saudi Population. *Cureus,* 14**,** e30695.

WEBER, C., MEILER, S., DÖRING, Y., et al. 2011. CCL17-expressing dendritic cells drive atherosclerosis by restraining regulatory T cell homeostasis in mice. *J Clin Invest,* 121**,** 2898-910.

WELCH, W. J. 2008. Angiotensin II-dependent superoxide: effects on hypertension and vascular dysfunction. *Hypertension,* 52**,** 51-6.

WILKERSON, M. J. 2012. Principles and applications of flow cytometry and cell sorting in companion animal medicine. *Vet Clin North Am Small Anim Pract,* 42**,** 53-71.

WILLIAMS, B., POULTER, N. R., BROWN, M. J., et al. 2004. British Hypertension Society guidelines for hypertension management 2004 (BHS-IV): summary. *Bmj,* 328**,** 634-40.

WILMINK, A. B., FORSHAW, M., QUICK, C. R., et al. 2002. Accuracy of serial screening for abdominal aortic aneurysms by ultrasound. *J Med Screen,* 9**,** 125-7.

WU, H., SMITH, M., MILLENSON, M. M., et al. 2003. Contribution of flow cytometry in the diagnosis of cutaneous lymphoid lesions. *J Invest Dermatol,* 121**,** 1522-30.

WU, Q. Q., YAO, Q., HU, T. T., et al. 2022. Tax1 banding protein 1 exacerbates heart failure in mice by activating ITCH-P73-BNIP3-mediated cardiomyocyte apoptosis. *Acta Pharmacol Sin,* 43**,** 2562-2572.

XAUS, J., MIRABET, M., LLOBERAS, J., et al. 1999. IFN-gamma up-regulates the A2B adenosine receptor expression in macrophages: a mechanism of macrophage deactivation. *J Immunol,* 162**,** 3607-14.

XU, C., LIU, X., YU, L., et al. 2023. CD147 monoclonal antibody attenuates abdominal aortic aneurysm formation in angiotensin II-Infused apoE(-/-) mice. *Int Immunopharmacol,* 122**,** 110526.

XUE, B., PAMIDIMUKKALA, J. & HAY, M. 2005. Sex differences in the development of angiotensin II-induced hypertension in conscious mice. *Am J Physiol Heart Circ Physiol,* 288**,** H2177-84.

XUE, B., PAMIDIMUKKALA, J., LUBAHN, D. B., et al. 2007. Estrogen receptor-alpha mediates estrogen protection from angiotensin II-induced hypertension in conscious female mice. *Am J Physiol Heart Circ Physiol,* 292**,** H1770-6.

YANG, D., ZHANG, Y., NGUYEN, H. G., et al. 2006. The A2B adenosine receptor protects against inflammation and excessive vascular adhesion. *J Clin Invest,* 116**,** 1913-23.

YAO, Y., CAO, Y., XU, Y., et al. 2023. CARMA3 Deficiency Aggravates Angiotensin II-Induced Abdominal Aortic Aneurysm Development Interacting Between Endoplasmic Reticulum and Mitochondria. *Can J Cardiol,* 39**,** 1449-1462.

ZERNECKE, A., BIDZHEKOV, K., ÖZÜYAMAN, B., et al. 2006. CD73/Ecto-5′-Nucleotidase Protects Against Vascular Inflammation and Neointima Formation. *Circulation,* 113**,** 2120-2127.

ZIMMERMAN, M. A., BABAN, B., TIPTON, A. J., et al. 2015. Chronic ANG II infusion induces sex-specific increases in renal T cells in Sprague-Dawley rats. *Am J Physiol Renal Physiol,* 308**,** F706-12.

13. Acknowledgements

A big thank you goes to the entire Molecular Cardiology Department. I am deeply thankful to Prof. Dr. rer. nat. Ulrich Flögel and Dr. rer. nat. Pascal Bouvain for entrusting me with the opportunity to conduct this research. Their support and belief in my abilities have been instrumental in shaping my academic journey. Thank you, dear Uli, for your support, especially during the first couple of months, and for helping me figure things out. PD Dr. rer. nat. Sebastian Temme also helped structure our work and ensure we were well-prepared for everything, consistently being critical, which only ensured the quality of the publication and the work done was excellent.

Pascal, thank you for everything. Thank you for always being there and for constantly supporting and guiding me through all the experiments and the writing of this thesis. Pascal, Patricia, Timo, and Bodo definitely made the atmosphere much better and helped me through tough times, assisting me in figuring everything out.

I thank Prof. Dr. med. dent. Petra C. Gierthmühlen for her constant support and for always pushing me to reach my full potential. I would also like to thank the whole prosthodontics team for their amazing support and the lovely atmosphere.

Dear Shery and Amir: I love you with all my heart. I know that you sacrificed a lot and invested in me. You allowed me to travel abroad to receive the best education and constantly supported me, even though it was hard for you to send your only child away. I hope that I can make you proud. I hope that I have also made my grandparents proud, although they are not here to witness what I have achieved.

I would also like to thank all of my friends who have supported me over the past few years. Thank you, Barbara, for assisting me and always providing help. Thank you, Carol, for keeping me company throughout my experiments.

Finally, I would like to express my gratitude to God for providing me with the strength, guidance, and perseverance needed to complete this journey. I love you, Lord, my strength. The Lord is my rock, my fortress, and my deliverer; my God is my rock, in whom I take refuge, my shield, and the horn of my salvation, my stronghold. (Psalms 18:1-2)